

# Time-varying Credibility, Anchoring and the Fed's Inflation Target

Max Diegel

School of Business & Economics

Discussion Paper

Economics

2022/9

# Time-varying Credibility, Anchoring and the Fed's Inflation Target\*

Max Diegel<sup>†</sup>

November 2022

## Abstract

This paper analyzes the time-varying credibility of the Fed's inflation target in an empirical macro model with asymmetric information, where the public has to learn about the actual inflation target from the Fed's interest rate policy. To capture the evolving communication strategy of the Fed, I allow the learning rule and the structural shock variances to change across monetary policy regimes. I find that imperfect credibility is pronounced during the Volcker Disinflation and to a lesser extent in the aftermath of the 2008 Financial Crisis. The announcement of the 2% target in 2012 did not affect the learning rule strongly but reduced the variance of transitory monetary policy shocks. The results caution against equating long-term inflation expectations of professionals with the perceived inflation target.

*JEL-Classification:* C11, C32, D83, D82, E31, E52

*Keywords:* signal extraction problem, credibility, inflation target, unobserved components, VAR

---

\*Financial support from the Deutsche Forschungsgemeinschaft (DFG) via the project *The Anchoring of Inflation Expectations* is gratefully acknowledged. I thank Geraldine Dany-Knedlik, Emanuel Gasteiger, Helmut Lütkepohl, Dieter Nautz, Mathias Trabandt and Tomasz Woźniak as well as the participants of the 2021 IAAE Annual Conference, the 2021 EEA Annual Conference, 13th RCEA Bayesian Econometrics Workshop and the doctoral Seminar in Empirical Macroeconomics at FU Berlin for useful discussions and comments.

<sup>†</sup>Affiliation: Freie Universität, Berlin

“A fuller understanding of the public’s learning rules would improve the central bank’s capacity to assess its own credibility, to evaluate the implications of its policy decisions and communications strategy.” Bernanke (2007)

## 1 Introduction

Central banks, like the Federal Reserve Bank (Fed), interpret price stability as inflation rates being close to an implicit or explicit inflation target. Thus, to achieve their inflation target, a central bank should ideally convey that it is credible in fulfilling its mandate of price stability. However, credibility is fragile and, once lost, can be costly to re-establish, as argued forcefully by Goodfriend (2004) for example. Therefore, monitoring the state of credibility at all times is indispensable.

Over most of the postwar period, the exact inflation target of the Fed was unknown to the public and probably time-varying. Therefore, the inflation target perceived by the public may sometimes deviate from the actual inflation target, creating a *credibility gap*. To help anchor public perceptions at, and strengthen the credibility of its target, the Fed has changed its communication strategy significantly since the early 1960s. For example, to foster understanding of the policy actions taken to reduce the high inflation rates of the late 1970s, “on October 6, 1979, the Fed broke sharply with its tradition of saying little in public about its actions” (Goodfriend 2007, p. 51) and explained them to a wider public. In January 2012, the Federal Open Market Committee (FOMC) announced the numerical inflation target of 2 percent for the annual inflation rate of the Personal Consumption Expenditure (PCE) index. Later, it redefined the target to be an *average* inflation target. Hence, even official target announcements can be subject to change. Moreover, they do not necessarily eliminate asymmetric information and imperfect credibility. For example, Coibion et al. (2020) find that, in the US, 60% of survey respondents among firms and 40% among households said they do not know what the Fed’s inflation target was. Therefore, the target perceived by the public need not automatically coincide with the officially announced inflation target by the central bank. Modeling the Fed’s inflation target as time-varying and not directly observable by the public may still be an accurate representation of the Fed’s monetary policy, even after 2012 and especially for the purpose of gauging potentially imperfect credibility.<sup>1</sup>

---

<sup>1</sup>Despite the official inflation target, Shapiro and Wilson (2019) find that the Fed more likely has targeted a rate of inflation that is slightly lower than the announced 2%, even after 2012. Moreover, average inflation targeting implies a certain degree of time-variation in the inflation target because the central may temporarily aim for inflation above or below 2%.

As pointed out in the lead quote by Bernanke (2007), knowledge of the public learning mechanism is important for assessing credibility and the impact of different communication strategies. Therefore, the aim of this paper is to contribute to a better understanding of the time-varying credibility of the Fed’s inflation target by estimating how the public learns about the inflation target from the Fed’s monetary policy.

**This paper.** The starting point of this paper is the learning mechanism of Kozicki and Tinsley (2005). In their model, the monetary policy rate is set by a Taylor rule with an unobservable and time-varying inflation target  $\pi_t^*$ . Due to asymmetric information, the public has to solve signal extraction problem to learn about the Fed’s inflation target. As a result, it updates the perceived target  $\pi_t^P$  in response to the observed interest rate policy of the central bank. Since  $\pi_t^*$  and  $\pi_t^P$  need not coincide, the model allows for a precise notion of imperfect credibility, the credibility gap. This paper then extends the analysis of Kozicki and Tinsley (2005) along three important dimensions.

First, I derive the learning rate that is optimal from the central bank’s perspective, thus providing an important benchmark for assessing empirical estimates of the learning rate. To that end, I propose the expected squared credibility gap at medium- to long horizons as an indicator of the degree of de-anchoring of  $\pi_t^P$  from  $\pi_t^*$ . This de-anchoring indicator naturally summarizes two key aspects of anchoring: Persistence and variance of the credibility gap. In the spirit of Jorgensen and Lansing (2022), the optimal learning rate is then found by minimizing this de-anchoring indicator. However, in contrast to the literature where agents learn from inflation surprises instead of monetary policy, a learning rate of zero is generally not optimal because it implies that the perceived target is unrelated to the inflation target.<sup>2</sup> Therefore, the derived optimal rate adds an interesting new perspective on the relation between learning and anchoring. As a result of the non-zero optimal learning rate, a response of the perceived target to monetary policy can be desirable because it helps to anchor public long-term inflation beliefs at the actual inflation target, as suggested also by the SVAR evidence in Diegel and Nautz (2021).

Second, I allow for breaks in the structural shock variances and the learning rate across US monetary policy regimes. Kozicki and Tinsley restrict the shock variances and the learning rate to be constant. However, the literature demonstrates that changes in shock variances are important to fit the evolution of the Fed’s monetary policy framework through

---

<sup>2</sup>When agents learn from inflation surprises and not from monetary policy, any change in their long-term inflation belief is considered undesirable and, thus, the degree of anchoring increases the smaller the learning rate is; see e.g. Jorgensen and Lansing (2022), Gáti (2022), Carvalho et al. (2022) and Lansing (2009).

the postwar period; see e.g. Primiceri (2005), Sims and Zha (2006), and Belongia and Ireland (2016). The dates of the regime changes are motivated by narrative historical evidence of Goodfriend (2004, 2007), the 2012 announcement of the 2% target, and findings of the structural VAR literature; see e.g. Brunnermeier et al. (2021). Since the optimal learning rate depends on the shock variances, different monetary regimes may also imply different optimal learning rates. To capture the effect of the changes to the Fed’s communication strategy on agent’s learning behavior, I allow the learning rate to vary across regimes as well. To the best of my knowledge, this is the first paper to estimate a non-constant learning rate that links public perceptions directly to the inflation target. This allows to check whether the announcement has had the desired effect: In that case, it should reduce the de-anchoring indicator by moving the learning rate of the public closer to the optimal value.<sup>3</sup>

Third, to estimate the Fed’s actual inflation target  $\pi_t^*$  and perceived inflation target  $\pi_t^P$  from US macro data, I generalize the precision based formulas for Bayesian estimation and model comparison of univariate correlated unobserved components models of Grant and Chan (2017) to the multivariate case. This generalization enables the use of precision based methods of Chan and Jeliazkov (2009) that are computationally more efficient than algorithms based on the Kalman filter and smoother. Moreover, the precision based methods directly deliver smoothed estimates that are best suited for the purpose of recovering historical relationships. Another advantage is that the Bayesian approach allows to explicitly incorporate prior beliefs on structural parameters and the trajectories of the unobserved components. For example, it is straightforward to explicitly account for the implicit prior belief that  $\pi_t^*$  should be *close* to 2% from 2012 onwards.<sup>4</sup>

**Results.** The model is estimated on US macro data from 1962Q1 to 2018Q3. The best fitting model allows for five breaks in the variances and the learning rate. Interestingly, the variances of shocks to  $\pi_t^*$  and  $\pi_t^P$  show different patterns of variation across the regimes, a finding that would have been ruled out by the assumption of equal variances by Kozicki and Tinsley.

---

<sup>3</sup>Other studies that estimate a constant learning rate are Erceg and Levin (2003) and Del Negro and Eusepi (2011). Carvalho et al. (2022) and Mertens and Nason (2020) estimate time-varying updating parameters for the inflation trend but their analysis omits an explicit role of the monetary policy and the inflation target, which are crucial for gauging credibility.

<sup>4</sup>Kozicki and Tinsley (2005) estimate the model with ML methods and report filtered estimates of  $\pi_t^*$  and  $\pi_t^P$  from the Kalman filter with no bands for inference. Following Kim and Kim (2022), Bayesian techniques should be preferred over maximum likelihood estimation for unobserved components models because they allow for overcoming the so-called ‘pile-up’ problem that can lead to a bias in the estimates of variances of the unobserved components.

The estimates for  $\pi_t^*$  and  $\pi_t^P$  indicate that imperfect credibility is an important feature to fit the evolution of the Fed’s monetary policy. Imperfect credibility was particularly important in the Volcker Disinflation due to the slow adjustment of agent’s perception after the shift to a lower inflation target, and to a lesser extent in the aftermath of the 2008 Financial Crisis. A model with perfect credibility, i.e.  $\pi_t^* = \pi_t^P$  for all  $t$ , is strongly rejected by the data.

The estimated level of the Fed’s inflation target  $\pi_t^*$  is close to 2% even before the 2012 announcement and it remains there since then. Re-estimating the model under an additional prior that restricts  $\pi_t^*$  to be ‘close’ to 2% does not deteriorate the model fit significantly. However, the de-anchoring indicator improves after the announcement. While the learning rate increases marginally, this increase is too small to contribute significantly to the improvement in anchoring. Instead, the improvement in anchoring is driven predominantly by a reduction of the variance of the transitory monetary policy shock, indicating that the Fed has followed its policy rule more closely since the announcement.

Moreover, the perceived target and observed long-term inflation expectations should not be equated directly, even though both capture similar economic concepts. A Bayesian model comparison shows that using long-term inflation expectations from the Survey of Professional Forecasters (SPF) as an imperfect measurement of the perceived target as in Chan et al. (2018) leads to a substantial deterioration in model fit.

**Outline.** The next section presents the learning mechanism of Kozicki and Tinsley, which serves as a starting point. It then proceeds to derive the optimal learning rate and implications for the evolution of the credibility gap and the degree of anchoring of the perceived target to the Fed’s actual target. Section 3 embeds the learning mechanism into a multivariate correlated unobserved components model and derives analytical expressions for Bayesian estimation and model comparison in a precision based framework. Section 4 presents the results of the baseline estimation and alternative specifications to assess the importance of imperfect credibility. Section 5 summarizes and concludes.

## 2 An empirical macro model with asymmetric information

To assess the time-varying credibility of the Fed’s inflation target I build on the asymmetric information model by Kozicki and Tinsley (2005). This section briefly revisits the learning

mechanism of their model. The main components are the monetary policy rule and the learning rule that updates the perceived inflation target. The subsequent subsection derives results of the model for credibility and the optimal learning rate.

## 2.1 The learning mechanism of Kozicki and Tinsley (2005)

Kozicki and Tinsley assume that monetary policy sets the nominal interest rate  $i_t$  according to a Taylor-type feedback rule in response to deviations of the annual inflation rate  $\bar{\pi}_t^4$  from the current value of the inflation target  $\pi_t^*$  and to a measure of the output gap  $g_t - \bar{g}$ . Moreover, it smooths past interest rate deviations  $i_{t-1}$  from the equilibrium level  $\bar{i}_{t-1}$ . The monetary policy rule reads

$$i_t = \bar{i}_t + \rho(i_{t-1} - \bar{i}_{t-1}) + \phi_{\pi,t}(\bar{\pi}_t^4 - \pi_t^*) + \phi_y(g_t - \bar{g}) + \varepsilon_t^{MP}, \quad \varepsilon_t^{MP} \sim N(0, \sigma_{MP}^2) \quad (1)$$

with  $\bar{i}_t = rr + \pi_{t-1}^P$ . (2)

The equilibrium level of the nominal rate  $\bar{i}_t$  is determined by a long-term Fisher-type relation where  $rr$  denotes the natural real rate and  $\pi_{t-1}^P$  is the perceived inflation target from the previous period. As is common in the literature on time-varying inflation targets,  $\pi_t^*$  follows an exogenous random walk, see e.g. Ireland (2007) and Cogley et al. (2010).<sup>5</sup>

$$\pi_t^* = \pi_{t-1}^* + \varepsilon_t^*, \quad \varepsilon_t^* \sim N(0, \sigma_\star^2) \quad (3)$$

While the monetary policy shock  $\varepsilon_t^{MP}$  only has a transitory effect in the policy interest rate, the target shock  $\varepsilon_t^*$  has a permanent effect.

Asymmetric information enters the model through the assumption that agents outside the central bank do not directly observe either the current value of the Fed's inflation target or the transitory shock. To form beliefs about the inflation target, which is the perceived inflation target  $\pi_t^P$ , agents have to solve a signal extraction problem. This involves forming expectations about the policy rate  $i_t^e$  and updating the perceived target  $\pi_t^P$  according to the

---

<sup>5</sup>Here, I deviate from the original model in two aspects. First, I do not include a 'Volcker dummy' in the law of motion for  $\pi_t^*$  to account for the large monetary policy shift that occurred between 1979 and 1983. Instead, changes in monetary policy are captured by allowing for changes in the variances of the shocks. For the Volcker Disinflation, this has the advantage that, while also allowing for larger target changes, this special regime can also be reflected in a larger variance of temporary monetary policy shocks, due to non-borrowed reserves targeting. Second, Kozicki and Tinsley allow the inflation target to react to temporary cost-push shocks, which seems implausible for most of the sample period. Moreover, since this is not at the heart of the current analysis, I abstract from this feature and assume that the inflation target is a purely exogenous random walk as in (3).

surprise  $i_t - i_t^e$ . Since  $\pi_t^*$  is unknown, agents use their latest value of  $\pi_{t-1}^P$  to form interest rate expectations. Thus, agents' one period ahead expected level of the interest rate is given by

$$i_t^e = \bar{i}_t + \rho(i_{t-1} - \bar{i}_{t-1}) + \phi_\pi(\bar{\pi}_t^A - \pi_{t-1}^P) + \phi_y(g_t - \bar{g})$$

After observing the actual level of the interest rate set via (1), agents' forecast error can be decomposed into contributions of transitory and permanent monetary policy components according to

$$i_t - i_t^e = \phi_\pi(\pi_{t-1}^P - \pi_t^*) + \varepsilon_t^{MP}. \quad (4)$$

If monetary policy is more contractionary than expected, the decomposition in (4) implies that the corresponding forecast error  $i_t - i_t^e > 0$  can be attributed to either a positive transitory monetary policy shock  $\varepsilon_t^{MP}$  or to agents' perceived target being higher than the actual inflation target, i.e.  $\pi_{t-1}^P - \pi_t^* > 0$ . Since both  $\varepsilon_t^{MP}$  and  $\pi_t^*$  are unobservable, agents do not know the source of their forecast error. However, they can adjust their perceived target according to size and direction of the forecast error. Following Kozicki and Tinsley, I assume that agents employ the following learning rule to update the perceived target

$$\pi_t^P = \pi_{t-1}^P - \delta(i_t - i_t^e) + \varepsilon_t^P, \quad \varepsilon_t^P \sim N(0, \sigma_P^2). \quad (5)$$

The learning rate  $\delta$  governs the relative weight that agents attach to new information in the expectation formation process. It can also be interpreted as the amount of attention that agents devote to monetary policy actions. If monetary policy is more contractionary than expected, agents revise  $\pi_t^P$  downward. The perceptions shock  $\varepsilon_t^P$  is an exogenous source of variation in  $\pi_t^P$  and allows for deviations from the learning rule. I deviate from Kozicki and Tinsley (2005) in that I do not impose the restriction  $\sigma_P^2 = \sigma_\star^2$  that was originally made for technical reasons but is hard to justify on economic grounds. The Bayesian estimation allows for replacing this restriction with a reasonable prior that still allows the two variances to be different.<sup>6</sup>

---

<sup>6</sup>As I am additionally allowing for different volatility regimes in the estimation, relaxing this restriction is even more important because it would *a priori* imply the same variance changes in target- and perceived target shocks in each regime.

Substituting (4) into (5) yields the law of motion for  $\pi_t^P$  as

$$\pi_t^P = (1 - \delta\phi_\pi)\pi_{t-1}^P + \delta\phi_\pi\pi_t^* - \delta\varepsilon_t^{MP} + \varepsilon_t^P. \quad (6)$$

If  $\phi_\pi > 0$  and  $\delta > 0$ , (6) implies that  $\pi_t^P$  is cointegrated one for one with the inflation target  $\pi_t^*$  with adjustment coefficient  $\phi_\pi\delta$  and perceptions will eventually converge to the Fed's target in the absence of shocks. For the observed data, this implies that  $\pi_t^*$  is the common trend of inflation  $\pi_t$  and the monetary policy interest rate  $i_t$ .

## 2.2 The credibility gap

The asymmetric information structure of the model prevents a first-best outcome of a perfectly credible inflation target  $\pi_t^* = \pi_t^P$  with zero variance for all  $t$ . To overcome asymmetric information in practice, central banks use their communication with the public as an additional tool for achieving credibility for their inflation targets. To that end, the communication strategies are often subject to change, while the general monetary policy framework remains largely unchanged. However, a change in the communication strategy should affect the weight of monetary policy in the public perceptions formation process, i.e. the learning rate  $\delta$ . In fact, the learning rate  $\delta$  can achieve a second-best outcome that is associated with minimum volatility and persistence of deviations of  $\pi_t^P$  from  $\pi_t^*$ . This section first defines the credibility gap  $\pi_t^P - \pi_t^*$  and then derives a value for the learning rate  $\delta_{t,s}^*$  that is conditionally optimal from a central bank point of view that seeks to minimize expected credibility gaps for horizons  $s = 1$  and  $s = \infty$ . These two cases allow to illustrate the intuition of optimal learning and serve as benchmarks for interpreting the empirically estimated learning in section 4.

The model allows a law of motion for credibility, defined as „the difference between the policymaker's plan and the public's beliefs about those plans” Cukierman and Meltzer (1986, p.1106). This definition corresponds to the deviation of the perceived target from the Fed's actual target  $\pi_t^P - \pi_t^*$ , that is bad credibility drives a wedge between  $\pi_t^*$  and  $\pi_t^P$ . To stress that larger magnitudes of  $|\pi_t^P - \pi_t^*|$  imply weaker credibility, it is referred to as the *credibility gap*. Subtracting  $\pi_t^*$  from (6) and inserting (3) yields the law of motion for the credibility gap:<sup>7</sup>

$$\pi_t^P - \pi_t^* = (1 - \delta\phi_\pi)(\pi_{t-1}^P - \pi_{t-1}^*) + \varepsilon_t^P - \delta\varepsilon_t^{MP} - (1 - \delta\phi_\pi)\varepsilon_t^* \quad (7)$$

---

<sup>7</sup>For the VECM describing the evolution  $\pi_t^*$  and  $\pi_t^P$ , this reformulation corresponds to the more general transformation in Carvalho and Harvey (2005, p.278) that uses eigenvectors and eigenvalues.

Again, if  $0 < \phi_\pi \delta < 1$ , the credibility gap converges to zero in absence of shocks implying that  $\pi_t^P$  is anchored at  $\pi_t^*$  *in the long run* in the sense of the long-run anchoring criterion of ?. For the remainder of this section, assume that this condition is satisfied. The estimation results show that the upper bound is empirically not binding. Given that  $\pi_t^P$  is anchored in the long run, the volatility and persistence of the credibility gap are two aspects a central bank might be concerned about.<sup>8</sup>

### 2.3 Optimal learning

The volatility and persistence of the credibility gap are naturally summarized by expected squared deviations of  $\pi_{t+s}^P$  from  $\pi_{t+s}^*$  at a medium- to long-term horizon  $s$ . To emphasize the role of these aspects for the degree of anchoring of  $\pi_t^P$  to  $\pi_t^*$ , those deviations are referred to as the *de-anchoring indicator*  $DAI_{t,s}$ , see Definition 2.3. [The De-Anchoring Indicator] Conditional on the information set as of period  $t$ , denoted  $\mathcal{I}_t$ , the degree of de-anchoring of  $\pi_{t+s}^P$  from  $\pi_{t+s}^*$   $s$  periods into the future is measured by

$$DAI_{t,s} := \text{E} \left[ \left( \pi_{t+s}^P - \pi_{t+s}^* \right)^2 \middle| \mathcal{I}_t \right]$$

Given a set of monetary policy coefficients, the rate of learning  $\delta$  plays a central role for the  $DAI_{t,s}$ . Therefore, a central bank that seeks to maintain credibility in the medium to long term prefers a value  $\delta_{t,s}^*$  that minimizes  $DAI_{t,s}$ :

$$\delta_{t,s}^* = \underset{\delta \in (0, \frac{1}{\phi_\pi})}{\text{argmin}} \quad DAI_{t,s}. \quad (8)$$

Since  $DAI_{t,s}$  is the long-run variance of the credibility gap when  $s \rightarrow \infty$ , for this case the problem resembles the criterion for optimal learning proposed by Lansing (2009). The value  $\delta_{t,s}^*$  is optimal for a central bank that chooses the Taylor rule coefficient  $\phi_\pi$  based on considerations about the trade-off between inflation and output stabilization and maximizes anchoring subject to that policy rule. The announcement of the 2% inflation target by the Federal Reserve can be understood as such an attempt to maximize anchoring of long-term inflation expectations *conditional* on the monetary policy regime already in place. If such communication tools have the desired anchoring-effect, they should move  $\delta$  closer to  $\delta_{t,s}^*$ .

Using the law of motion for the credibility gap allows to derive an analytical expression

---

<sup>8</sup>This is akin to the criteria considered for the anchoring of long-term inflation expectations, see e.g. Doh and Oksol (2018).

for the  $DAI_{t,s}$ , see Proposition 2.3. The proof is contained in Appendix A. [Model implied  $DAI_{t,s}$ ] The credibility gap in equation (7) implies

$$DAI_{t,s} = (\pi_t^P - \pi_t^*)^2 (1 - \delta\phi_\pi)^{2s} + \left(1 - (1 - \delta\phi_\pi)^{2s}\right) \frac{(\delta^2\sigma_{MP}^2 + \sigma_*^2 (1 - \delta\phi_\pi)^2 + \sigma_P^2)}{1 - (1 - \delta\phi_\pi)^2} \quad (9)$$

For the case  $s = 0$ , where the central bank does not care about future deviations of the perceived target from  $\pi_t^*$ ,  $DAI_{t,s}$  collapses to the squared current credibility gap. By contrast, if the central bank cares also about future deviations, the degree of de-anchoring is not reflected adequately by only the current credibility gap. As central banks are forward looking,  $s = 0$  is hardly an empirically relevant choice. Therefore, this section proceeds to analyze the degree of anchoring for the more plausible case of  $s > 0$ .

In principle, the horizon  $s$  can be chosen to match the central bank's definition of the 'medium term'. However, the mechanics of the  $DAI_{t,s}$  are best illustrated by two extreme cases  $s \rightarrow \infty$  and  $s = 1$  which allow to simplify  $DAI_{t,s}$  considerably, see Corollary 2.3. [Special cases for  $DAI_{t,s}$ ] For  $s \rightarrow \infty$  and  $s = 1$ ,  $DAI_{t,s}$  simplifies to

$$DAI_\infty = \frac{\delta^2\sigma_{MP}^2 + (1 - \delta\phi_\pi)^2\sigma_*^2 + \sigma_P^2}{1 - (1 - \delta\phi_\pi)^2} \quad (10)$$

and

$$DAI_{t,1} = (\pi_t^P - \pi_t^*)^2 (1 - \delta\phi_\pi)^2 + \delta^2\sigma_{MP}^2 + \sigma_*^2 (1 - \delta\phi_\pi)^2 + \sigma_P^2. \quad (11)$$

Inserting the expression for  $DAI_\infty$  from (10) into the expression for  $DAI_{t,s}$  in (9) yields

$$DAI_{t,s} = (\pi_t^P - \pi_t^*)^2 (1 - \delta\phi_\pi)^{2s} + \left(1 - (1 - \delta\phi_\pi)^{2s}\right) DAI_\infty. \quad (12)$$

From this, it is easy to see that  $DAI_{t,s}$  converges to  $DAI_\infty$  monotonically as  $s \rightarrow \infty$ . Moreover,  $DAI_{t,s}$  approaches  $DAI_\infty$  from above (below) if the current squared credibility gap is larger (smaller) than  $DAI_\infty$ . Given long run anchoring, both  $DAI_\infty$  and  $DAI_{t,1}$  are decreasing in the Taylor rule coefficient on inflation  $\phi_\pi$  due to the decline in persistence of the credibility gap. This intuitive finding is also in line with the theory of anchored inflation expectations of Gáti (2022), who concludes that a more aggressive central bank reaction to inflation deviations anchors long-run inflation beliefs. Moreover, both de-anchoring indicators are increasing in the variances  $\sigma_P^2$ ,  $\sigma_{MP}^2$  and,  $\sigma_*^2$ .

Corollary 2.3 summarizes the effect of a change in  $\delta$  on  $DAI_\infty$  and  $DAI_{t,1}$ . Due to

the nature of asymmetric information, a higher learning rate does not necessarily improve anchoring. This is because an increase in  $\delta$  has two opposite effects. On the one hand, it improves anchoring by reducing the persistence of the credibility gap, reflected in the right hand side of the conditions in Corollary 2.3. On the other hand, a higher  $\delta$  also increases the impact of transitory monetary policy shocks on the credibility gap, represented by the left hand side of the conditions. Thus, a higher  $\delta$  only improves anchoring if the reduction in persistence dominates the higher impact of the monetary policy shock on the credibility gap. Moreover, the strength of these opposite effects differs between the horizons  $s$ . For example, for  $s \rightarrow \infty$ , the reduction in persistence is more likely to dominate if  $\sigma_t^P$  is large. For  $s = 1$ , this is the case if the current credibility gap is large. Given  $0 < \phi_\pi$  and  $0 < \delta \leq \frac{1}{\phi_\pi}$ , for  $s \rightarrow \infty$  we have

$$\frac{\partial \text{DAI}_\infty}{\partial \delta} \begin{cases} \leq 0, & \text{for } \delta^2 \sigma_{MP}^2 \leq (\sigma_*^2 + \sigma_P^2) (1 - \delta \phi_\pi) \\ > 0, & \text{for } \delta^2 \sigma_{MP}^2 > (\sigma_*^2 + \sigma_P^2) (1 - \delta \phi_\pi) \end{cases}$$

and for  $s = 1$

$$\frac{\partial \text{DAI}_{t,1}}{\partial \delta} \begin{cases} \leq 0, & \text{for } \delta^2 \sigma_{MP}^2 \leq \left( \sigma_*^2 + (\pi_t^P - \pi_t^*)^2 \right) \phi_\pi (1 - \delta \phi_\pi) \\ > 0, & \text{for } \delta^2 \sigma_{MP}^2 > \left( \sigma_*^2 + (\pi_t^P - \pi_t^*)^2 \right) \phi_\pi (1 - \delta \phi_\pi) \end{cases}$$

[The optimal learning rates] For  $s \rightarrow \infty$  and  $s = 1$ ,

$$\delta_\infty^* = \frac{\sqrt{(\sigma_*^2 + \sigma_P^2) (\phi_\pi^2 \sigma_*^2 + \phi_\pi^2 \sigma_P^2 + 4\sigma_{MP}^2)} - \phi_\pi (\sigma_*^2 + \sigma_P^2)}{2\sigma_{MP}^2} \quad (13)$$

and

$$\delta_{t,1}^* = \frac{\phi_\pi \left( (\pi_t^P - \pi_t^*)^2 + \sigma_*^2 \right)}{\phi_\pi^2 \left( (\pi_t^P - \pi_t^*)^2 + \sigma_*^2 \right) + \sigma_{MP}^2}. \quad (14)$$

solve the problem in (8). Solving (8) yields the optimal learning rates, see Proposition 2.3. The proof is contained in Appendix A. The optimal learning rates  $\delta_\infty^*$  and  $\delta_{t,1}^*$  depend differently on the shock variances and the Taylor rule parameter. Thus, to judge whether a higher or lower value of  $\delta$  is needed to improve anchoring at a specific horizon, it is useful to compare any estimated value for  $\delta$  with both extreme cases  $\delta_\infty^*$  and  $\delta_{t,1}^*$ . For example, in the case of a perfectly credible inflation target at time  $t$ , i.e.  $\pi_t^P - \pi_t^* = 0$ , and a central

bank that follows the Taylor rule almost exactly, i.e.  $\sigma_{MP}^2 \rightarrow 0$ , the optimal learning rate  $\delta_{i,1}^*$  approaches its upper bound  $\frac{1}{\phi\pi}$  under long-run anchoring. The maximum learning speed is optimal in this case because every forecast error agents make in forecasting the interest rate  $i_t$  originates from a change in  $\pi_t^*$ . If the central bank would not follow the Taylor rule in setting its interest rate policy, i.e.  $\sigma_{MP}^2 \rightarrow \infty$ , the interest rate contains no information about the inflation target and, consequently, a learning rate of close to zero would be optimal. However, in the empirically relevant case, where the central bank follows the Taylor rule approximately, a modestly positive learning rate is optimal.

In contrast, models that assume long-term inflation beliefs are formed based on inflation surprises exclusively imply that a learning rate of close to zero maximizes anchoring because every movement in long-term inflation beliefs is undesirable by definition; see for example Carvalho et al. (2022). The results of this section show that, when agents learn from monetary policy instead of inflation surprises, a non-zero learning rate can be optimal.

## 2.4 US Monetary policy regimes and the learning rate

To estimate a meaningful learning parameter  $\delta$ , it is necessary to capture monetary policy adequately in the estimation. The SVAR literature on US monetary policy largely agrees that the variances of the structural shocks have changed across the different monetary regimes, while the coefficients of the policy reaction function remained remarkably stable in post war data (Sims and Zha 2006; Belongia and Ireland 2016). Changes in volatilities are of particular interest for the anchoring of the perceived target to the actual target because the optimal learning rate and the de-anchoring indicators depend on the volatilities. To account for potential changes in volatilities, I follow Brunnermeier et al. (2021) and allow the structural shock variances to change between break dates suggested by the literature.

In addition to the break dates of Brunnermeier et al. (2021), I allow for a break in January 2012 for the announcement of the official 2% inflation target. Intuitively, the variances of changes in the inflation target  $\sigma_\star^2$  and deviations from the Taylor rule  $\sigma_{MP}^2$  may have decreased after the announcement.

Even under constant variances the optimal  $\delta_{i,1}^*$  is time-varying because it depends on the current value of the credibility gap. In contrast,  $\delta_\infty^*$  is constant because it “sees through” current credibility gaps that are only temporary under long-run anchoring. However, time-variation in the variances of the shocks can imply time-variation in  $\delta_\infty^*$ . Since the optimal learning rates depends on the shock variances, I also allow the learning rate  $\delta$  to change at

the break dates.<sup>9</sup>

Studies focusing on learning from inflation surprises document time-variation in the estimated learning rates, see e.g. Carvalho et al. (2022), Jorgensen and Lansing (2022) and Gáti (2022). In contrast, the learning mechanism of Kozicki and Tinsley assumes that agents learn from monetary policy surprises. To the best of my knowledge, the present study is the first to estimate the time-varying learning gain in a monetary policy-based learning mechanism, and hence, adds an important perspective the literature. For example, if the 2012 announcement had the desired effect on credibility and anchoring, it should have led to a decline in the variance of the target- and transitory monetary policy shocks and shifted the learning rate  $\delta$  closer to its optimal value.

### 3 Bayesian estimation

To estimate the inflation target  $\pi_t^*$  and the perceived inflation target  $\pi_t^P$ , the structural equations of the previous section are mapped to state space form. This form yields a multivariate unobserved components model with correlated errors. The vector of  $n = 3$  macroeconomic variables  $y_t = [g_t, \pi_t, i_t]'$  consists of a measure of the output gap  $g_t$ , inflation  $\pi_t$  and the central bank interest rate  $i_t$ . The data vector  $y_t$  is decomposed into the  $r = 2$  common trends, collected in the vector  $\tau_t = [\pi_t^P, \pi_t^*]'$ . The deviations of the variables from the trends are denoted  $c_t = [\hat{g}_t, \hat{\pi}_t, \hat{i}_t]'$  and are assumed to be stationary. The full observation equation linking the observables to the state vectors is

$$y_t = \tilde{\gamma}_y + \Gamma_0 \tau_t + \Gamma_1 \tau_{t-1} + c_t \quad (15)$$

with

$$\tilde{\gamma}_y = \begin{bmatrix} \bar{g} \\ 0 \\ rr \end{bmatrix} \quad \Gamma_0 = \begin{bmatrix} 0 & 0 \\ 1 & 0 \\ 0 & 0 \end{bmatrix} \quad \Gamma_1 = \begin{bmatrix} 0 & 0 \\ 0 & 0 \\ 1 & 0 \end{bmatrix}$$

where  $\bar{g}$  is the constant average of the output gap that might be different from zero in a particular sample period and  $rr$  is the real interest rate. Note that only  $\pi_t^P$  enters directly into the inflation equation; see second row of  $\Gamma_0$ . Moreover,  $\pi_t^P$  appears with a lag in the interest rate equation; see third row of  $\Gamma_1$ . The state equations governing the evolution of

---

<sup>9</sup>The breaks in the signal-to-noise ratio due to breaks in variances imply changes in the optimal learning gain not only from the anchoring analysis, but also from a Kalman filter, i.e. optimal forecasting, perspective.

the cycles  $c_t$  and the trends  $\tau_t$  are

$$Ac_t = B_1c_{t-1} + \dots + B_p c_{t-p} + \lambda_0\tau_t + \dots + \lambda_q\tau_{t-q} + e_t, \quad e_t \sim N(0, \Sigma_t) \quad (16)$$

$$\tau_t = F_t\tau_{t-1} + J_t e_t + O_t u_t, \quad u_t \sim N(0, \Omega_t) \quad (17)$$

where  $u_t = [\varepsilon_t^P, \varepsilon_t^*]'$  and  $e_t = [\varepsilon_t^g, \varepsilon_t^\pi, \varepsilon_t^{MP}]'$ . The  $t$  subscript of the diagonal variance matrices  $\Sigma_t$  and  $\Omega_t$  indicates the dependence on the US monetary policy regimes. The coefficient matrices  $F_t$ ,  $J_t$ , and  $O_t$  also have a  $t$  subscript because they depend on the learning rate  $\delta$ , which is also allowed to vary across the regimes. For brevity, the exact definitions the model matrices are relegated to Appendix B. Suffice to mention that  $A$  is lower triangular with unit diagonal. The coefficients in the  $n$ th row of  $A$ , the  $B_j$ s and the  $\lambda_j$ s obey linear restrictions such that the interest rate equation equals the Taylor rule in (1). After substituting the decomposition  $\pi_t = \pi_t^P + \hat{\pi}_t$  from (15) into the Taylor rule, the  $\lambda_j$  matrices account for how  $\pi_t^*$  and  $\pi_{t-i}^P$  for  $i = 0, \dots, 3$  affect interest rate deviations  $\hat{i}_t$ . Since  $\pi_t^*$  and  $\pi_{t-i}^P$  do not enter any other equation for  $c_t$ , the  $\lambda_j$  contains only zeros elsewhere. Equation (17) stacks laws of motion for  $\pi_t^*$  and  $\pi_t^P$  in (3) and (6). Since the cycle shocks  $e_t$  show up in the equations for  $\tau_t$  and  $c_t$ , I refer to the model defined by equations (15)-(17) as multivariate correlated unobserved components (MCUC) model.

### 3.1 Priors

I use natural conjugate priors where possible to allow for an efficient estimation. This means normal distributions as priors for all slope coefficients and initial values of the unobserved components, and inverse gamma distributions for all variances. For the shock variances of the stationary cycles  $\sigma_g^2$ ,  $\sigma_\pi^2$ , and  $\sigma_{MP}^2$ , I use inverse gamma distributed priors with a mean of 0.5 and 6 degrees of freedom. For the shock variances of the trends  $\sigma_x^2$  and  $\sigma_P^2$ , I use inverse gamma distributed priors with a smaller mean of 0.05 and 5 degrees of freedom. The smaller mean is justified because changes in the inflation target or the perceived target can be expected to be smaller on average than business cycle shocks. Still, the prior is not overly restrictive. For example, at the prior mean, 95% of the changes in  $\pi_t^*$  are smaller than 0.44 in absolute value. For the Taylor rule coefficients  $\rho$ ,  $\phi_\pi$ , and  $\phi_g$ , I use informative normal priors with mean 0.7, 0.45, and 0.15 and variances of 0.05 each that are reminiscent of priors for these parameters from Smets and Wouters (2007). The use of informative priors is justified because these are structural parameters with a clear economic meaning. The other slope coefficients in the  $B_i$  matrices of all other cyclical equations have unspecific and wide normal priors with zero mean and unit variance. For the learning rate  $\delta$ , I use a

beta prior of the form  $\delta \sim \text{beta}(a_\delta, b_\delta)$  with  $a_\delta = 4$  and  $b_\delta = 16$  implying a mean of 0.2. This prior restricts  $0 < \delta < 1$  and ensures that the long-run anchoring criterion is obeyed. While the lower bound also ensures the correct sign for  $\delta$ , the upper bound is not empirically relevant.

### 3.2 Posterior simulation and marginal likelihood computation

The model is estimated using Bayesian methods. The use of Bayesian methods has the advantage that prior beliefs on structural parameters and the trajectories of unobserved components can be explicitly taken into account. Moreover, the different priors on the variances of the cycle and trend shocks add to the identification of the unobserved components without imposing hard restrictions.<sup>10</sup>

The posterior of the model is simulated with a Gibbs sampler. The Gibbs sampler approximates the posterior by iteratively generating draws from the conditional posterior distribution of the unknown parameters and the states  $\tau_t$ , reminiscent of an Expectation Maximization algorithm. For the purpose of recovering in-sample relations, smoothed estimates of  $\tau_t$  are most appropriate because they use all the available sample information. The most efficient way to draw  $\tau_t$  from its smoothing distribution is by use of the precision sampler of Chan and Jeliaskov (2009). Unfortunately, the formulas for the precision sampler for correlated unobserved components models are only available for the univariate case, see Grant and Chan (2017). Therefore, to estimate the MCUC model, I generalize the formulas to the multivariate case. The individual steps of the algorithm are detailed in Appendix D. To ensure convergence of the Gibbs sampler I discard the first 5000 draws as burn-in sample. All results are based on the 20000 draws following the burn-in.

To efficiently compute the marginal likelihood, required for Bayesian model comparison, I also generalize the analytical computation of the integrated likelihood of Grant and Chan (2017) to the multivariate case. The marginal likelihood is obtained by numerically integrating out the unknown coefficients from the integrated likelihood. This requires many evaluations of the integrated likelihood, which is greatly facilitated by a closed form expression that can be evaluated quickly. Using this analytical expression, I obtain the marginal likelihood via the cross-entropy method of Chan and Eisenstat (2015). The cross-entropy method is an importance sampling procedure that requires specifying distribution

---

<sup>10</sup>Kozicki and Tinsley (2005) estimate the model with ML methods and report filtered estimates of  $\pi_t^*$  and  $\pi_t^P$  from the Kalman filter with no bands for inference. Following Kim and Kim (2022), Bayesian techniques should be preferred over maximum likelihood estimation for unobserved components models because they allow for overcoming the so-called ‘pile-up’ problem that can lead to a bias in the estimates of variances of the unobserved components.

families for the proposal densities for all parameters. Following Chan and Eisenstat (2015), I use proposal densities from the same families as the prior densities for each coefficient. I use 10 batches with 10000 draws each to compute the marginal likelihood. Since the cross entropy method yields a numerical approximation, there is also a small error. To gauge the approximation error, I compute a numerical standard error (NSE) for the marginal likelihood estimates across the 10 batches.

For brevity, the formulas and derivations are contained in C. The formula for the integrated likelihood of the MCUC can also be used in maximum likelihood estimation.

## 4 Credibility of the Fed’s inflation target from 1962 to 2018

I estimate the model on three quarterly US time series from 1962Q1 to 2018Q3: the output gap  $g_t$  obtained from the Congressional Budget Office, the annualized quarterly inflation rate of the Personal Consumption Expenditure  $\pi_t$ , and the Fed Funds rate  $i_t$ . From 2009 to 2015, while the zero lower bound was binding,  $i_t$  is equal to the shadow rate of Wu and Xia (2016), which captures the unconventional monetary measures taken during that time.<sup>11</sup> Before interpreting the results, I determine the monetary policy break dates out of the candidate break dates that yield the best fit.

### 4.1 Determining the monetary policy break dates

To fit the US data and find the most relevant break dates, I compare the marginal likelihoods from models estimated with different sets of break dates from Brunnermeier et al. (2021) plus a break in January 2012 for the inflation target announcement. Table 1 confirms that variance changes are a relevant feature to fit the data. The best fitting model with the largest marginal likelihood has five break dates in total; see row 6. The regime breaks refer to the first month of the new regime. The five breaks that yield the best fit mark the beginnings of the the Stagflation period in January 1973, the regime change in October 1979 shortly after Paul Volcker was appointed chairman of the Fed, the end of the monetary targeting in January 1983, the onset of the financial crisis in January 2008, and the announcement of the inflation target in January 2012.

---

<sup>11</sup>All series are obtained from economic database of the St. Louis Fed, FRED. Only the shadow rate, which is obtained from Cyntia Wu’s homepage at <https://sites.google.com/view/jingcynthiawu/shadow-rates>.

Table 1: Log marginal likelihoods for various sets of regime break dates

Start date of new regime						
Jan-1973	Oct-1979	Jan-1983	Jan-1990	Jan-2008	Jan-2012	$\log ML$ ( <i>NSE</i> )
						-965.6 (0.67)
					✓	-960.29 (0.42)
	✓	✓			✓	-927.14 (1.5)
✓	✓	✓			✓	-922.64 (1.11)
✓	✓	✓	✓		✓	-926.32 (1.29)
✓	✓	✓		✓	✓	-907.93 (1.22)
✓	✓	✓	✓	✓	✓	-913.73 (1.27)

*Notes: Log marginal likelihoods are computed using the cross-entropy method of (Chan and Eisenstat 2015) with 10 runs of 10000 importance sampling draws each. Numerical standard error (NSE) across the 10 runs in parenthesis. Strength of evidence for differences in log ML according to Kass and Raftery (1995):  $0 < \Delta \log ML < 1$ : not worth mentioning,  $1 < \Delta \log ML < 3$ : positive,  $3 < \Delta \log ML < 5$ : strong,  $5 < \Delta \log ML$ : very strong. Additional break dates of Belongia and Ireland (2016) in Jan-2000 and Jan-1984 instead of Jan-1983 did not increase the fit log ML.*

Allowing for these breaks in volatilities and the learning rate, the constant Taylor rule coefficients also have the expected sign; see Table 2. Moreover, the implied long-run response to inflation deviations from target exceeds unity and obeys the Taylor principle. The smoothing coefficient  $\rho$  is relatively low. Since time-variation in  $\pi_t^*$  and imperfect credibility, two elements that are absent in conventional specifications, also capture persistence in the interest rate, this Taylor rule requires only a smaller smoothing parameter.

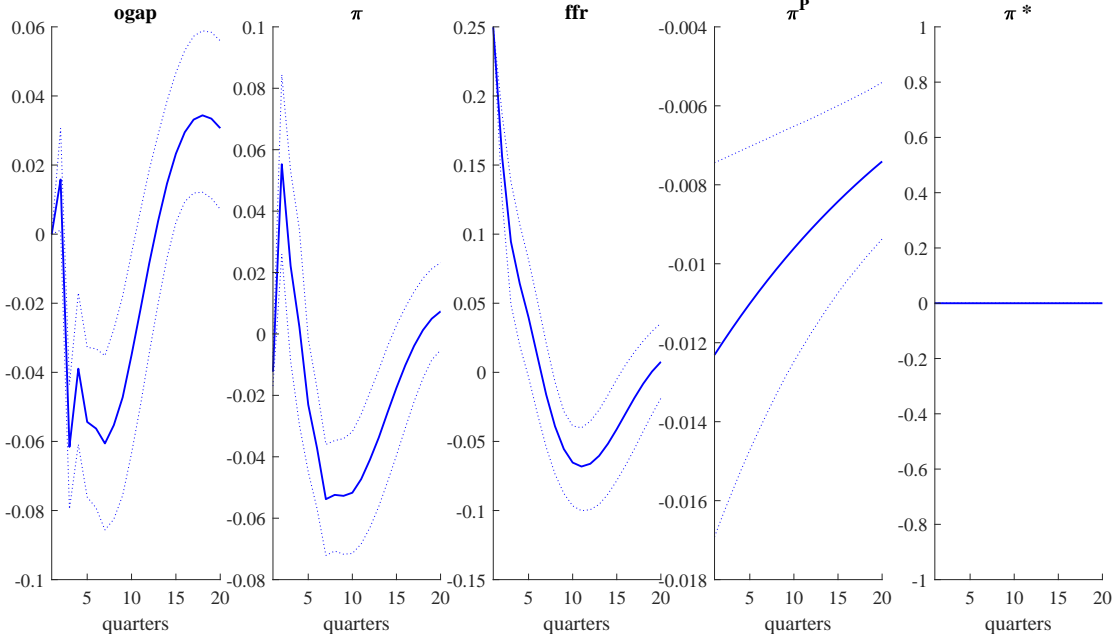
The typical response to a temporary monetary policy  $\varepsilon_t^{MP}$  shock implied by the model is also plausible, see Figure 1. A 25 basis points hike in the fed funds rate leads to a decline in the output gap and a delayed decrease in inflation after a small price puzzle. The perceived target decreases modestly after the shock and, by construction, the inflation target remains

Table 2: Taylor rule coefficients of the best fitting model.

	$\phi_g$	$\phi_\pi$	$\rho$
mean (5% 95%)	0.25 (0.14 0.36)	0.51 (0.33 0.68)	0.63 (0.5 0.76)

Notes: The posterior means of the implied long-run responses to inflation and the output gap are  $\frac{\phi_\pi}{1-\rho} = 1.11$  and  $\frac{\phi_g}{1-\rho} = 0.70$ .

Figure 1: Impulse responses to a monetary policy shock



Notes: Posterior means (solid) 16% and 84% posterior quantiles (dashed lines). The shock is normalized to increase the fed funds rate by 25 basis points. To show the typical response implied by the model, the impulse responses are averaged over the values of the learning rate  $\delta$  from the different monetary policy regimes.

constant.<sup>12</sup>

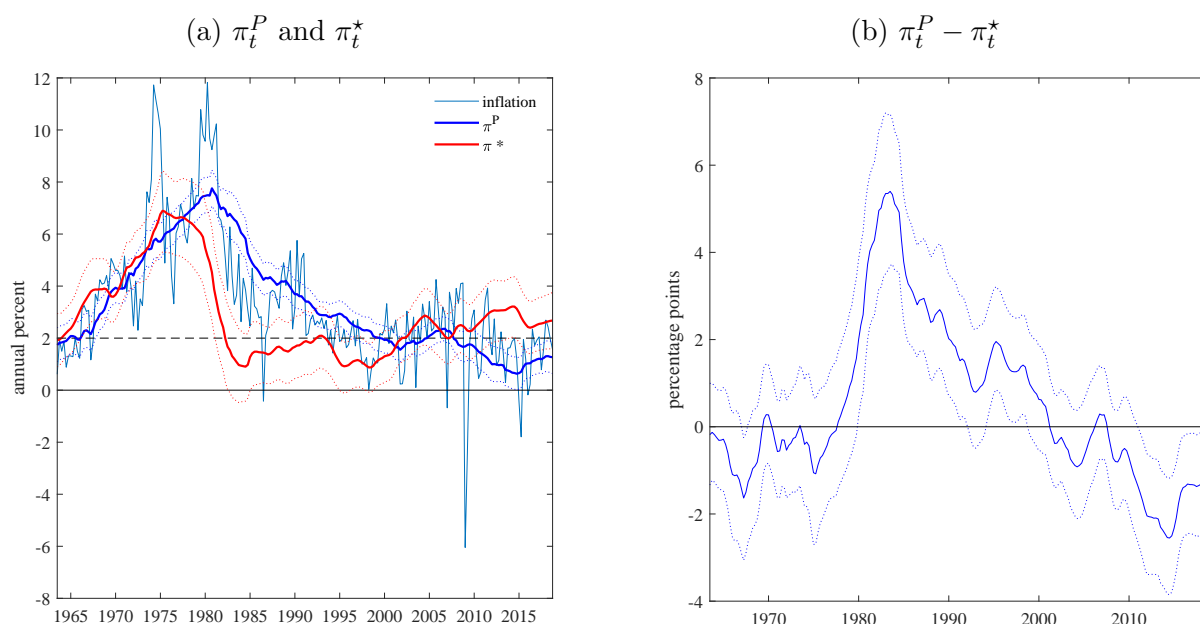
Since the Taylor rule and the impact of the monetary policy shock of the best fitting model are plausible, the results in the following sections are based on the same set of regime breaks. The next section considers the potential time-varying credibility.

## 4.2 The time-varying credibility of $\pi_t^*$

Figure 2 shows the estimated paths for  $\pi_t^P$  and  $\pi_t^*$  and the credibility gap. It is obvious that  $\pi_t^P$  and  $\pi_t^*$  do not coincide over large parts of the sample and, thus, that credibility

<sup>12</sup>Note the inflation decreases on impact because the perceived target  $\pi^P$  decreases on impact.

Figure 2: The evolution of  $\pi_t^P$ ,  $\pi_t^*$  and the credibility gap



Notes: Horizontal lines indicate zero (solid) and 2% (dashed). Dotted lines are 16% and 84% posterior quantiles.

has not always been perfect. In fact, imperfect credibility was a problem during the Volcker Disinflation, and the Great Moderation, and, to a lesser extent, in the aftermath of the 2008 Financial Crisis. Until the mid-1970s, both,  $\pi_t^P$  and  $\pi_t^*$  increase steadily. Moreover, this rise is largely simultaneous indicated by the insignificant credibility gap during that period. Through the lens of the Taylor rule, a rise of  $\pi_t^*$  reflects the fact the Fed has not rigorously enforced low inflation with the ‘go-stop’-type policy; see e.g. Goodfriend (2004). In the late 1970s and early 1980s, the so-called Volcker Disinflation, an apparent regime change takes place:  $\pi_t^*$  drops sharply to below 2% reflecting the Fed taking on the fight against high inflation. In contrast to the preceding simultaneous rise of  $\pi_t^P$  and  $\pi_t^*$ , the drop in  $\pi_t^*$  clearly leads the decline in inflation and the gradual decline of  $\pi_t^P$  through the Great Moderation period. This results in a large positive credibility gap. The 68% probability bands for the credibility bands contain zero again in the late 1990s.

Note that since the drop of  $\pi_t^*$  in the early 1980s, 2% is always contained in the 68% credibility bands.<sup>13</sup> This suggests that the 2012 announcement was a mere change in

<sup>13</sup>However,  $\pi_t^*$  from Kozicki and Tinsley (2005) drops into negative territory at the end of the Volcker Disinflation just to increase sharply thereafter. While this excessively sharp drop can be due to their ‘Volcker dummy’ in the law of motion for  $\pi_t^*$ , their estimate is much more volatile than the one in Figure 2, also in periods other than 1979Q4 to 1982Q4. This is reflected in their relatively large estimate for  $\sigma_{\pi^*}^2 = 0.23$  which is more than twice the size of the maximum of 0.11 that I obtain outside the period from 1973Q1 to 1979Q3; see Table 3.

communication rather than a shift in the actual inflation target. However, in the aftermath of the Financial Crisis, the posterior mean of  $\pi_t^*$  increases to above 2%. This rise can be attributed partly to the unconventional monetary policy measures taken, which are reflected in the shadow rate. It may, despite the announced target, indicate a higher tolerance for inflation vis-a-vis other goals of the Fed. At the same time  $\pi_t^P$  declines below 2%. As a result, zero remains outside the probability band of the credibility gap through the sample end in 2018Q3. However, as shown in the previous sections, a central bank that cares about future credibility should also take into account the regime dependent volatilities and the learning rate because they determine the degree of de-anchoring at medium- to long horizons. Therefore, the next section considers those aspects jointly.

### 4.3 Learning and de-anchoring in different monetary regimes

The left panel of Figure 3 plots the estimated and optimal learning rates  $\delta_{t,1}^*$  and  $\delta_\infty^*$  along with the estimated  $\delta$  across the regimes. Several stark observations emerge:

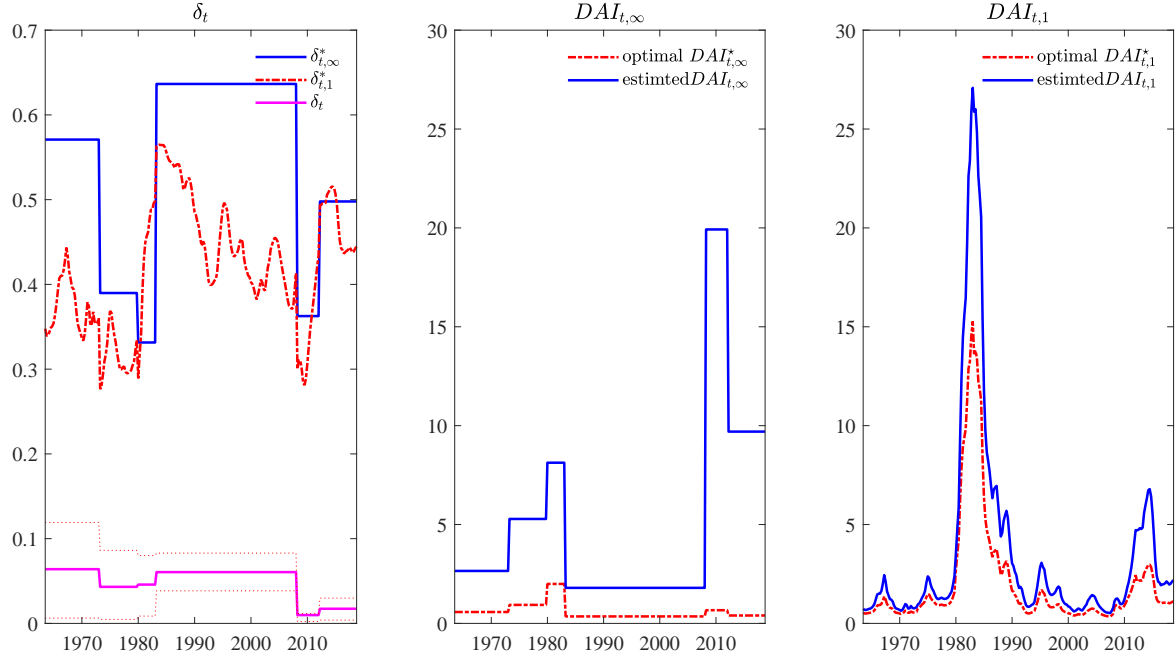
First, the estimated  $\delta$  is lower than both optimal learning rates, in the entire sample period, indicating that agents update their beliefs too slowly.

Second, the profile of  $\delta$  follows the profile of the optimal rates  $\delta_\infty^*$  and  $\delta_{t,1}^*$  across the regimes. For example, all three drop under the Financial Crisis regime. The drop of  $\delta_\infty^*$  is mostly driven by the increase of  $\sigma_{MP}^2$  from 2008Q1 to 2011Q4 while the other variances that determine  $\delta_\infty^*$ , i.e.  $\sigma_P^2$  and  $\sigma_\star^2$ , remain almost unchanged; see Table 3. The increase in  $\sigma_{MP}^2$  most likely reflects the modest decline in the interest rate compared to the sharp temporary drop in inflation. The fact that  $\delta$  also drops along with  $\delta_\infty^*$  in this period suggests that agents were well aware of this.

Third, the learning rate was higher before the Great Recession than after. This finding is generally in line with findings of Carvalho et al. (2022), who report a lower learning rate in the more recent period. Also, Jorgensen and Lansing (2022) find that the learning rate drops even further after the Great Recession. However, the implications are different: In their models, agents learn from *inflation surprises* and, thus, a lower learning rate is associated with better anchoring of inflation beliefs because shocks to inflation will not lead big movements in long-term beliefs. In contrast, when agents learn from monetary policy, a learning rate of close to zero is not optimal because the link between the actual target and the perceived target becomes weaker. This is reflected in both  $DAI_{t,1}$  and  $DAI_\infty$ , in the middle and right panel, peaking in the aftermath of the 2008 Financial Crisis. Hence, considering only the effect of inflation surprises on agent's long-term inflation beliefs might

overstate the degree of anchoring.

Figure 3: Estimated and optimal learning rate, and de-anchoring indicators



Notes: The left panel shows mean of the optimal learning rates  $\delta_{t,1}^*$  (solid blue) and  $\delta_{t,\infty}^*$  (dashed red) implied by the posterior distributions of the parameters, as well as the posterior mean (solid magenta) of the estimated learning rate  $\delta$  with 68% credibility bands (dotted magenta) for the various monetary regimes. The middle and right panels show the posterior mean of the  $DAI_{t,1}$  and  $DAI_{t,\infty}$  evaluated at the actual learning rate (solid blue) and  $DAI_{t,1}^*$  and  $DAI_{t,\infty}^*$  evaluated at the respective optimal learning rates (dashed red).

Table 3: Regime dependent learning rate and shock variances

Regime	$\delta$	$\sigma_g^2$	$\sigma_\pi^2$	$\sigma_{MP}^2$	$\sigma_P^2$	$\sigma_\star^2$
1972Q4	0.06 (0.01 0.12)	0.61 (0.49 0.74)	0.76 (0.58 0.94)	0.34 (0.25 0.43)	0.06 (0.04 0.09)	0.10 (0.05 0.14)
1973Q1 to 1979Q3	0.04 (0.00 0.09)	0.77 (0.59 0.95)	1.71 (1.26 2.17)	0.90 (0.60 1.19)	0.07 (0.03 0.10)	0.11 (0.04 0.16)
1979Q4 to 1982Q4	0.05 (0.01 0.08)	0.72 (0.51 0.92)	0.91 (0.61 1.21)	2.48 (1.66 3.28)	0.06 (0.03 0.08)	0.29 (0.09 0.46)
1983Q1 to 2007Q4	0.06 (0.04 0.08)	0.24 (0.21 0.28)	1.12 (0.95 1.28)	0.18 (0.14 0.22)	0.04 (0.02 0.05)	0.07 (0.04 0.10)
2008Q1 to 2011Q4	0.01 (0.00 0.01)	0.64 (0.46 0.82)	4.01 (2.91 5.08)	0.78 (0.45 1.10)	0.05 (0.03 0.08)	0.06 (0.03 0.08)
2012Q1 to 2018Q3	0.02 (0.00 0.03)	0.28 (0.21 0.34)	0.81 (0.61 1.01)	0.30 (0.21 0.39)	0.04 (0.03 0.06)	0.05 (0.03 0.08)

Notes: Reported figures are posterior means and 16% and 84% quantiles in parentheses.

To better understand the dynamics of the  $DAI_{t,1}$  and  $DAI_{t,\infty}$  through the entire sample, it is helpful to also take into account the changing volatilities in Table 3. In line with

the narrative account of the Great Inflation, the estimated de-anchoring indicators both peak in the early 1980s and then decline. These peaks are driven by the high volatilities of temporary monetary policy, and inflation target shocks,  $\sigma_{MP}^2$  and  $\sigma_{\star}^2$ .

Both de-anchoring indicators peak a second time in the 2008 recession. For  $DAI_{t,\infty}$ , the peak in the Volcker Disinflation is lower than the peak in the 2008 Recession, whereas the opposite is true for  $DAI_{t,1}$ . Taken at face value,  $DAI_{t,\infty}$  would suggest that the de-anchoring was as severe as never before in 2008. However, this interpretation might be misleading because the  $DAI_{t,\infty}$  completely ignores the current credibility gap  $\pi_t^P - \pi_t^{\star}$ , which is much lower after the Financial Crisis than during the Volcker Disinflation. Therefore, a high value of  $DAI_{t,\infty}$  should *not* be confused with poor credibility. Rather, the increase in  $DAI_{t,\infty}$  signals that credibility is more vulnerable to *future* shocks. Therefore, it might be interpreted as an early warning indicator rather than a reflection of the current state. In contrast, the peak of  $DAI_{t,1}$  in the early 1980s is much higher than the peak after the Financial Crisis because it takes into account that credibility gap was much smaller after the crisis.

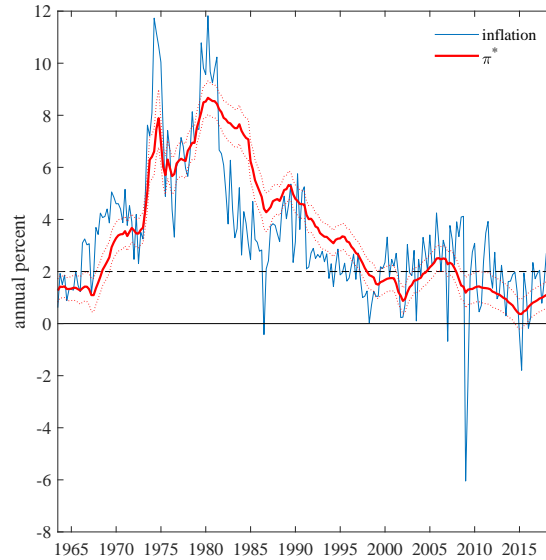
Finally, preventing  $\delta$  from becoming *too small* is more important than engineering the exact optimal value. This is due to the shape of the nonlinear mapping from the learning rate to the de-anchoring indicators. To see this, consider the de-anchoring indicators implied by the estimated parameters against the level of the indicators  $DAI_{t,\infty}^{\star}$  and  $DAI_{t,1}^{\star}$  that would prevail under the respective optimal learning rates, all else equal. The gap between the  $DAI_{t,\infty}$  and  $DAI_{t,1}$  and their optimal counterparts is small in the Great Moderation even though the deviation of  $\delta$  from  $\delta_{\infty}^{\star}$  is largest during this period. In contrast, the deviation of  $\delta$  from  $\delta_{\infty}^{\star}$  is much smaller when  $DAI_{t,\infty}$  reaches its maximum. This is because the de-anchoring indicator penalizes very low learning rates over-proportionally. Thus, from a central bank's perspective, it might be more important that  $\delta$  is not too small, than that it is exactly at the optimal value. In line with this conclusion, Gáti (2022) finds that a cost-push shock has almost identical effects on the typical macro variables under a *strong* and a *weak* anchoring of expectations. By contrast, the same shock has a much more adverse effect under completely unanchored expectations.

Did the 2012 announcement improve anchoring? The decline of both,  $DAI_{t,\infty}$  and  $DAI_{t,1}$  after the 2012 supports this hypothesis. At the same time  $\delta$  recovers only marginally and cannot explain the decline in the de-anchoring indicators by itself. However, the volatility of the temporary monetary policy shock drops after the 2012 announcement, see Table 3. This drop most likely accounts for the bulk of the improvement in the anchoring.

## 4.4 The inflation target under perfect credibility

Asymmetric information prevents credibility from being perfect even when the learning rate is at its optimal value because agents can only imperfectly disentangle between temporary monetary policy shocks and inflation target shocks. What would the estimated path of  $\pi_t^*$  look like under perfect credibility? To answer this question, the model is re-estimated under perfect information which implies  $\pi_t^P = \pi_t^*$  for all  $t$ , while maintaining time-variation in  $\pi_t^*$ . Without asymmetric information  $\pi_t^*$  is the only common trend of inflation and the central bank interest rate. The implications of this restriction for the estimated path of  $\pi_t^*$  and the model fit allow for drawing conclusions about the empirical importance of imperfect credibility.<sup>14</sup>

Figure 4:  $\pi_t^*$  obtained under perfect credibility



Notes: Horizontal lines indicate zero (solid) and 2% (dashed). Dotted lines are 16% and 84% posterior quantiles.

The estimate of  $\pi_t^*$ , obtained under perfect credibility, reveals a counter intuitive feature: The decline of  $\pi_t^*$  during the Volcker Disinflation *lags* behind the decline of inflation, see Figure 4. This suggests that the inflation target follows the path of inflation sluggishly not the other way around. The literature estimating  $\pi_t^*$  under perfect credibility often finds the same counter intuitive feature, see e.g. Figure 3 of Castelnovo et al. (2014) for a direct

<sup>14</sup>Kozicki and Tinsley (2005) only compare their asymmetric information model with a model of perfect credibility and *constant*  $\pi_t^*$ , thus not allowing to draw conclusions about the statistical relevance of imperfect credibility alone. Moreover, they do not conduct a formal model comparison.

comparison.<sup>15</sup> However, this estimate of the inflation target is at odds with the view that the Volcker-Fed set out to reduce inflation already in 1979, when inflation was still very high as argued for example in Lindsey et al. (2013). Following this argument, the decline in the inflation target should *lead* the decline in inflation, as is the case in the baseline results; see Figure 2.

Moreover, a Bayesian model comparison clearly favors the baseline model against the perfect credibility model. The log marginal likelihood for the perfect credibility model is -970.21 with a numerical standard error of 0.39 against -907.93 for the baseline model; see Table 1.<sup>16</sup> The difference in log marginal likelihoods of approximately 62 is very strong evidence in favor of the baseline model with imperfect credibility according to the Kass and Raftery (1995) scale. Thus, the results strongly suggest that imperfect credibility is an important feature of US monetary policy throughout the postwar period.

In contrast, Del Negro and Eusepi (2011) find that rational expectations DSGE models with perfect information are preferred over asymmetric information specifications using a sample covering 1984 through 2008. However, this sample period excludes the Volcker Disinflation and the low-inflation period in the aftermath of the financial crisis, two periods where imperfect credibility appears to have been especially important according to the baseline model. Despite many other model differences, the sample period is probably an important driver of this contrasting result.

## 4.5 The 2012 announcement and SPF inflation expectations

This section explores implications of using additional information in form of the official target announcement or observed survey inflation expectations in the estimation of the model.

**A 2%-prior for  $\pi_t^*$ .** One may argue that, since the 2012 announcement, the random walk law of motion allows  $\pi_t^*$  to wander excessively in comparison to the implicit prior belief that the inflation target should be close to 2%. To take this implicit prior into account, an explicit prior on the path of  $\pi_t^*$  can be added to the model equations. Not only is this approach preferable for its transparency instead of discarding models with ‘implausible’ trajectories for  $\pi_t^*$  *a posteriori*, but it can also help disentangling movements of  $\pi_t^*$  and  $\pi_t^P$  in the estimation. From a classical perspective, such a prior can be viewed as a soft restriction

---

<sup>15</sup>Studies that estimate  $\pi_t^*$  under perfect credibility include Ireland (2007), Aruoba and Schorfheide (2011), Coibion and Gorodnichenko (2011), and Castelnuovo et al. (2014). An exception is Milani (2020) who obtains a nearly constant estimate for  $\pi_t^*$  under learning on the side of the central bank.

<sup>16</sup>The perfect credibility model is estimated with the same breaks as the baseline model.

on the estimated path for  $\pi_t^*$ . If not rejected by the data, such a restriction can lead to more economically plausible and precise estimates. The prior takes the following form

$$\begin{aligned} \pi_t^* &= \pi^A + \varepsilon_t^A, & \varepsilon_t^A &\sim N(0, s_A^2) \\ \Rightarrow \pi_t^* &\sim N(\pi^A, s_A^2) & \text{for } t > \text{January 2012} \end{aligned} \quad (18)$$

with  $\pi^A = 2$ .  $\pi_t^*$  can vary freely until January 2012 but the prior restricts time-variation thereafter. The standard deviation  $s_A$  controls the average size of deviations from the announcement  $\pi^A$  that are allowed under this prior. I set  $s_A = 0.1$  which implies  $P(1.8 < \pi_t^* < 2.2) \approx 0.95$ . Thus, most of the prior density mass of  $\pi_t^*$  is in a reasonably narrow interval around 2%.

**Using survey expectations for estimation of  $\pi_t^P$ .** Newer literature (e.g. Crump et al. 2018; Chan et al. 2018; Bańbura and van Vlodrop 2018; Del Negro et al. 2017) exploits data on long-run inflation expectations from surveys, denoted  $\pi_t^{LR}$ , in the estimation of the trend in inflation. Figure 5 confirms that there is a broad co-movement between 10y inflation expectations for the consumer price index (CPI) from the Philadelphia Fed’s Survey of Professional Forecasters and the estimated  $\pi_t^P$ . To refine the estimation and relate the model based perceived target to observed inflation expectations, long-term inflation expectations could be used as a noisy measurement of  $\pi_t^P$  via another observation equation in the spirit of Chan et al. (2018):

$$\begin{aligned} \pi_t^{LR} &= d_0 + d_1 \pi_t^P + \varepsilon_t^{LR}, & \varepsilon_t^{LR} &\sim N(0, \sigma_{LR}^2) \\ \Rightarrow \pi_t^{LR} &\sim N(d_0 + d_1 \pi_t^P, \sigma_{LR}^2) \end{aligned} \quad (19)$$

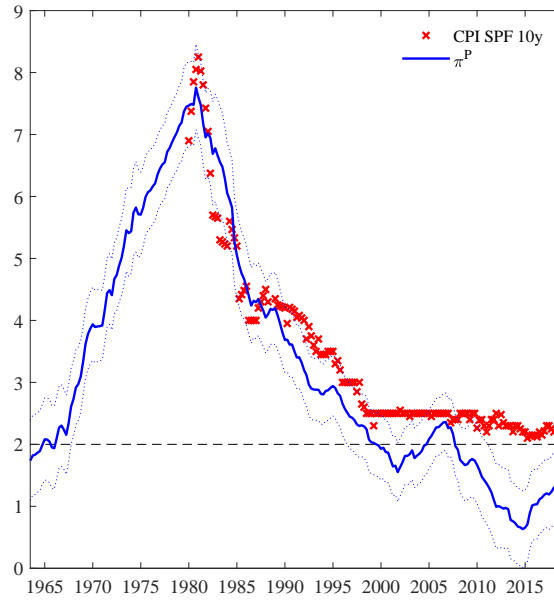
The coefficient  $d_0$  allows for a potential bias of  $\pi_t^{LR}$  with respect to  $\pi_t^P$  and  $d_1$  allows for different volatility of  $\pi_t^{LR}$  and  $\pi_t^P$ . A bias may arise because PCE and CPI differ on average by a constant amount. However, the dynamic properties of both series are hard to distinguish, supporting the use of CPI expectations as a measurement of the PCE based  $\pi_t^P$ .<sup>17</sup>

Table 4 compares the log marginal likelihoods of the baseline model with models using the 2%-prior in (18) and  $\pi_t^{LR}$  as in (19) as additional restrictions. Adding  $\pi_t^{LR}$  to the baseline model decreases the log ML by about 14 log points to  $-922.38$  indicating a strong deterioration of the fit to the macro data. Additionally restricting  $\pi_t^*$  leads to a decrease

---

<sup>17</sup>To relate PCE inflation to CPI long-run inflation expectations, Doh and Oksol (2018) rely on a rule of thumb that CPI is about 0.4 percentage points above PCE inflation on average.

Figure 5:  $\pi_t^P$  and SPF 10y CPI inflation expectations



Notes: Philadelphia Fed's SPF CPI 10y inflation expectations are extended backwards using the bi-annual series of long-term from the Blue Chip and Livingston Survey, also available from the Philadelphia Fed. The final series runs from 1979Q4 to 2018Q3.

Table 4: Log marginal likelihoods of models with restrictions on  $\pi_t^P$  and  $\pi_t^*$

sample	Restrictions on unobserved components			
	none (baseline)	only $\pi_t^*$	only $\pi_t^P$	$\pi_t^*$ and $\pi_t^P$
1962–2018	−907.93 (1.22)	−910.03 (0.69)	−922.38 (0.66)	−924.15 (1.10)
1962–2007	−721.69 (0.60)	—	−737.56 (0.75)	—

Note: Reported figures are log marginal likelihoods and numerical standard error in parenthesis, see notes of Table 1. To enable an ‘apples-to-apples’ comparison, the likelihoods are computed based only on the macro variables  $y_t$ . According to the best-fit, break dates for all models are in January 1973, October 1979, January 1983, January 2008, and January 2012. The restrictions on  $\pi_t^P$  and  $\pi_t^*$  are the 2%-prior and the use of  $\pi_t^{LR}$  as in (18) and (19), respectively.

of only 2 log points. Taking into account the numerical standard errors suggests that the deterioration in fit is not very significant. Similarly, the fit of the model with both additional restrictions is also much worse than the model only restricting  $\pi_t^*$  but not much worse than the model that only uses  $\pi_t^{LR}$ . Overall, there is strong evidence against using  $\pi_t^{LR}$  to restrict  $\pi_t^P$  but much less compelling evidence against restricting  $\pi_t^*$  to close to 2% after 2012.

## 5 Conclusion

This paper estimates how the public forms the long-term inflation beliefs by learning from the Fed’s interest rate policy, thereby contributing to a better understanding of drivers of the time-varying target credibility and the anchoring of public perceptions at the Fed’s inflation target. To enable an analysis of the role of learning for the anchoring of public perceptions, I propose a de-anchoring indicator that is motivated by asymmetric information about the Fed’s inflation target and derive an optimal learning rate that minimizes de-anchoring. In this model, a learning rate of zero is generally not optimal.

To apply the analysis to the US, I estimate the model on US postwar data from 1960 to 2018. To account for different monetary policy regimes, I allow for breaks in the variances and the learning rate. To estimate the model and enable Bayesian model comparison via the marginal likelihood, I derive precision based expressions for efficient state sampling and evaluation of the integrated likelihood.

Four main results emerge from the baseline estimation. First, imperfect credibility is an important feature of the joint evolution of US inflation and the Fed’s interest rate policy. A model that does not allow for imperfect credibility is clearly rejected by the data. Second, the optimal learning rate varies between 0.3 and 0.65 in the US postwar period. The profile of the estimated actual learning rate largely follows the the profile of the optimal rate. However, there is a substantial level shift: The public learns much too slowly compared to the optimal rate. Third, the degree of anchoring improves after the announcement of the 2% inflation target in 2012. This improvement is mainly driven by a reduction in the volatility of temporary monetary policy shocks. The learning rate increases slightly, but this has, if at all, only a small effect on the degree of anchoring. Fourth, despite the improved anchoring, the de-anchoring indicators remain elevated compared to the Great Moderation, indicating that credibility is more vulnerable to unfavorable shocks. Credibility could be made more robust if the Fed manages to increase the weight of monetary policy in agent’s belief formation process.

Finally, this model shows that a decline in the learning rate can also deteriorate the degree of anchoring of public perceptions to the actual inflation target. In contrast, a learning rate of zero maximizes anchoring in models where agents learn from inflation surprises instead of monetary policy. For future research it would be interesting to pin down the relative importance of these two sources of learning, especially since central banks around the world are confronted with above target inflation again since 2021.

## References

- Aruoba, S. B. and F. Schorfheide (2011). Sticky Prices versus Monetary Frictions: An Estimation of Policy Trade-Offs. *American Economic Journal: Macroeconomics* 3(1), 60–90.
- Bañbura, M. and A. van Vlodrop (2018). Forecasting with Bayesian Vector Autoregressions with Time Variation in the Mean. Tinbergen Institute Discussion Papers 18-025/IV, Tinbergen Institute.
- Belongia, M. T. and P. N. Ireland (2016). Money and Output: Friedman and Schwartz Revisited. *Journal of Money, Credit and Banking* 48(6), 1223–1266.
- Bernanke, B. S. (2007). Inflation Expectations and Inflation Forecasting. Speech, Monetary Economics Workshop of the National Bureau of Economic Research.
- Brunnermeier, M., D. Palia, K. A. Sastry, and C. A. Sims (2021). Feedbacks: Financial Markets and Economic Activity. *American Economic Review* 111(6), 1845–79.
- Carvalho, C., S. Eusepi, E. Mönch, and B. Preston (2022). Anchored Inflation Expectations. *American Economic Journal: Macroeconomics* (forthcoming).
- Carvalho, V. M. and A. C. Harvey (2005). Convergence in the Trends and Cycles of Euro-Zone Income. *Journal of Applied Econometrics* 20(2), 275–289.
- Castelnuovo, E., L. Greco, and D. Raggi (2014). Policy Rules, Regime Switches, and Trend Inflation: An Empirical Investigation for the United States. *Macroeconomic Dynamics* 18(4), 920–942.
- Chan, J. C. and E. Eisenstat (2015). Marginal Likelihood Estimation with the Cross-Entropy Method. *Econometric Reviews* 34(3), 256–285.
- Chan, J. C. and A. L. Grant (2015). Pitfalls of Estimating the Marginal Likelihood using the Modified Harmonic Mean. *Economics Letters* 131, 29–33.
- Chan, J. C. and A. L. Grant (2016). Fast Computation of the Deviance Information Criterion for Latent Variable models. *Computational Statistics and Data Analysis* 100, 847–859.
- Chan, J. C. and I. Jeliazkov (2009, January). Efficient simulation and integrated likelihood estimation in state space models. *International Journal of Mathematical Modelling and Numerical Optimisation* 1(1-2), 101–120.
- Chan, J. C. C., T. E. Clark, and G. Koop (2018). A New Model of Inflation, Trend Inflation, and Long-Run Inflation Expectations. *Journal of Money, Credit and Banking* 50(1), 5–53.
- Cogley, T., G. E. Primiceri, and T. J. Sargent (2010). Inflation-Gap Persistence in the US.

- American Economic Journal: Macroeconomics* 2(1), 43–69.
- Coibion, O. and Y. Gorodnichenko (2011). Monetary Policy, Trend Inflation, and the Great Moderation: An Alternative Interpretation. *American Economic Review* 101(1), 341–70.
- Coibion, O., Y. Gorodnichenko, S. Kumar, and M. Pedemonte (2020). Inflation Expectations as a Policy Tool? *Journal of International Economics* 124, 103297.
- Crump, R. K., S. Eusepi, and E. Moench (2018). The Term Structure of Expectations and Bond Yields. Technical Report 775, Federal Reserve Bank of New York.
- Cukierman, A. and A. H. Meltzer (1986). A Theory of Ambiguity, Credibility, and Inflation under Discretion and Asymmetric Information. *Econometrica* 54(5), 1099–1128.
- Del Negro, M. and S. Eusepi (2011). Fitting Observed Inflation Expectations. *Journal of Economic Dynamics and Control* 35(12), 2105–2131.
- Del Negro, M., D. Giannone, M. P. Giannoni, and A. Tambalotti (2017). Safety, Liquidity, and the Natural Rate of Interest. *Brookings Papers on Economic Activity* 48(1 (Spring)), 235–316.
- Diegel, M. and D. Nautz (2021). Long-Term Inflation Expectations and the Transmission of Monetary Policy Shocks: Evidence from a SVAR Analysis. *Journal of Economic Dynamics and Control* 130, 104192.
- Doh, T. and A. Oksol (2018). Has the Anchoring of Inflation Expectations Changed in the United States during the Past Decade? *Economic Review* (Q I), 31–58.
- Erceg, C. J. and A. T. Levin (2003). Imperfect Credibility and Inflation Persistence. *Journal of Monetary Economics* 50(4), 915–944.
- Gáti, L. (2022). Monetary policy and Anchored Expectations: An Endogenous Gain Learning Model. Working Paper 2685, European Central Bank.
- Goodfriend, M. (2004). Inflation Targeting in the United States? In *The inflation-targeting debate*, pp. 311–352. University of Chicago Press.
- Goodfriend, M. (2007). How the World Achieved Consensus on Monetary Policy. *Journal of Economic Perspectives* 21(4), 47–68.
- Grant, A. L. and J. C. Chan (2017). A Bayesian Model Comparison for Trend-Cycle Decompositions of Output. *Journal of Money, Credit and Banking* 49(2-3), 525–552.
- Ireland, P. N. (2007). Changes in the Federal Reserve’s Inflation Target: Causes and Consequences. *Journal of Money, Credit and Banking* 39(8), 1851–1882.
- Jorgensen, P. L. and K. J. Lansing (2022). Anchored Inflation Expectations and the Slope of the Phillips Curve. Working Paper 2019-27, Federal Reserve Bank of San Francisco.
- Kass, R. E. and A. E. Raftery (1995). Bayes factors. *Journal of the American Statistical Association*

- association* 90(430), 773–795.
- Kim, C.-J. and J. Kim (2022). Trend-Cycle Decompositions of Real GDP Revisited: Classical and Bayesian Perspectives on an Unsolved Puzzle. *Macroeconomic Dynamics* 26(2), 394–418.
- Kozicki, S. and P. A. Tinsley (2005). Permanent and Transitory Policy Shocks in an Empirical Macro Model with Asymmetric Information. *Journal of Economic Dynamics and Control* 29(11), 1985–2015.
- Kroese, D. P., J. C. Chan, et al. (2014). *Statistical Modeling and Computation*. Springer.
- Lansing, K. J. (2009). Time-Varying US Inflation Dynamics and the New Keynesian Phillips Curve. *Review of Economic Dynamics* 12(2), 304–326.
- Lindsey, D. E., A. Orphanides, R. H. Rasche, et al. (2013). The Reform of October 1979: How it happened and Why. *Federal Reserve Bank of St. Louis Review* 95(6), 487–542.
- Mertens, E. and J. M. Nason (2020). Inflation and Professional Forecast Dynamics: An Evaluation of Stickiness, Persistence, and Volatility. *Quantitative Economics* 11(4), 1485–1520.
- Milani, F. (2020). Learning and the Evolution of the Fed’s Inflation Target. *Macroeconomic Dynamics* 24(8), 1904–1923.
- Primiceri, G. E. (2005). Time Varying Structural Vector Autoregressions and Monetary Policy. *The Review of Economic Studies* 72(3), 821–852.
- Shapiro, A. H. and D. Wilson (2019, June). Taking the Fed at its Word: A New Approach to Estimating Central Bank Objectives using Text Analytics. Technical Report 2019-02, Federal Reserve Bank of San Francisco.
- Sims, C. A. and T. Zha (2006). Were There Regime Switches in US Monetary Policy? *American Economic Review* 96(1), 54–81.
- Smets, F. and R. Wouters (2007). Shocks and frictions in us business cycles: A bayesian dsge approach. *American economic review* 97(3), 586–606.
- Wu, J. C. and F. D. Xia (2016). Measuring the Macroeconomic Impact of Monetary Policy at the Zero Lower Bound. *Journal of Money, Credit and Banking* 48(2-3), 253–291.

## A Analytical Results

[Proof of Proposition 2.3] Let  $\pi_t^\dagger = \pi_t^P - \pi_t^*$  denote the credibility gap and its law of motion

$$\begin{aligned}\pi_t^\dagger &= \alpha \pi_{t-1}^\dagger + u_t, \quad u_t \sim N(0, \sigma_{u,t}^2) \\ \text{with } \alpha &= (1 - \delta_t \phi_\pi) \\ u_t &= \varepsilon_t^P - \delta_t \varepsilon_t^{MP} - (1 - \delta \phi_\pi) \varepsilon_t^* \\ \text{and } \sigma_{u,t}^2 &= \sigma_P^2 + \delta_t^2 \sigma_{MP}^2 + (1 - \delta \phi_\pi)^2 \sigma_*^2\end{aligned}$$

Iterating  $\pi_t^\dagger$  forward yields

$$\pi_{t+s}^\dagger = \alpha^s \pi_t^\dagger + \sum_{i=1}^s \alpha^{s-i} u_{t+s-i}.$$

Using this expression, the  $DAI_{t,s} = E \left[ \left( \pi_{t+s}^\dagger \right)^2 \middle| \mathcal{I}_t \right]$  can be written as

$$\begin{aligned}DAI_{t,s} &= \alpha^{2s} (\pi_t^\dagger)^2 + \sum_{i=1}^s \alpha^{2(s-i)} \sigma_u^2 \\ &= \alpha^{2s} (\pi_t^\dagger)^2 + \frac{1 - \alpha^{2s}}{1 - \alpha^2} \sigma_u^2 \\ &= (\pi_t^\dagger)^2 (1 - \delta \phi_\pi)^{2s} + \left( 1 - (1 - \delta \phi_\pi)^{2s} \right) \frac{(\delta^2 \sigma_{MP}^2 + \sigma_*^2 (1 - \delta \phi_\pi)^2 + \sigma_P^2)}{1 - (1 - \delta \phi_\pi)^2}\end{aligned}$$

[Proof of Proposition 2.3] For  $s \rightarrow \infty$

$$\frac{\partial DAI_\infty}{\partial \delta} = \frac{2(\delta^2 \sigma_{MP}^2 + (\sigma_*^2 + \sigma_P^2)(\delta \phi_\pi - 1))}{\delta^2 \phi_\pi (\delta \phi_\pi - 2)^2}$$

with  $\left. \frac{\partial DAI_\infty}{\partial \delta} \right|_{\delta=\delta_\infty^*} = 0$ . It remains to show that  $\frac{\partial^2 DAI}{\partial \delta^2} > 0$ , where

$$\frac{\partial^2 DAI_\infty}{\partial \delta^2} = - \frac{2(2\delta^3 \phi_\pi \sigma_{MP}^2 + (\sigma_*^2 + \sigma_P^2)(3\delta^2 \phi_\pi^2 - 6\delta \phi_\pi + 4))}{\delta^3 \phi_\pi (\delta \phi_\pi - 2)^3}.$$

The denominator of  $\frac{\partial^2 DAI_\infty}{\partial \delta^2}$  is negative for the admissible parameters space  $\delta \in (0, \frac{1}{\phi_\pi})$ . For admissible values of  $\delta$ , the nominator is positive if  $3(\delta \phi_\pi)^2 - 6\delta \phi_\pi + 4 > 0$ . This quadratic form is bounded from below by unity for  $\delta \phi_\pi = 1$  at the upper bound of the admissible parameter space. Therefore,  $\frac{\partial^2 DAI_t}{\partial \delta^2}$  is negative everywhere in the admissible parameter

space.

For  $s = 1$

$$\frac{\partial \text{DAI}_{t,1}}{\partial \delta} = 2(\pi_t^P - \pi_t^*)^2 \phi_\pi (\delta \phi_\pi - 1) + 2\delta \sigma_{MP}^2 + 2\phi_\pi \sigma_*^2 (\delta \phi_\pi - 1)$$

with  $\left. \frac{\partial \text{DAI}_{t,1}}{\partial \delta} \right|_{\delta=\delta_{t,1}^*} = 0$ . Furthermore, we have

$$\frac{\partial^2 \text{DAI}_{t,1}}{\partial \delta^2} = 2(\pi_t^P - \pi_t^*)^2 \phi_\pi^2 + 2\sigma_{MP}^2 + 2\phi_\pi^2 \sigma_*^2 > 0.$$

## B Model matrices

The full model is given by

$$y_t = \tilde{\gamma}_y + \Gamma_0 \tau_t + \Gamma_1 \tau_{t-1} + c_t \quad (20)$$

$$Ac_t = B_1 c_{t-1} + \dots + B_p c_{t-p} + \lambda_0 \tau_t + \dots + \lambda_q \tau_{t-q} + e_t, \quad e_t \sim N(0, \Sigma_t) \quad (21)$$

$$\tau_t = F_t \tau_{t-1} + J_t e_t + O_t u_t, \quad u_t \sim N(0, \Omega_t). \quad (22)$$

with diagonal variance matrices  $\Sigma_t = \text{diag}(\sigma_{g,t}^2, \sigma_{\pi,t}^2, \sigma_{MP,t}^2)$  and  $\Omega_t = \text{diag}(\sigma_{P,t}^2, \sigma_{*,t}^2)$ , and

$$\tilde{\gamma}_y = \begin{bmatrix} \bar{g} \\ 0 \\ rr \end{bmatrix} \quad \Gamma_0 = \begin{bmatrix} 0 & 0 \\ 1 & 0 \\ 0 & 0 \end{bmatrix} \quad \Gamma_1 = \begin{bmatrix} 0 & 0 \\ 0 & 0 \\ 1 & 0 \end{bmatrix}$$

$$A = \begin{bmatrix} 1 & 0 & 0 \\ a_{2,1} & 1 & 0 \\ -\phi_y & -\frac{\phi_\pi}{4} & 1 \end{bmatrix} \quad \lambda_0 = \begin{bmatrix} 0 & 0 \\ 0 & 0 \\ \frac{\phi_\pi}{4} & -\phi_\pi \end{bmatrix} \quad \lambda_i = \begin{bmatrix} 0 & 0 \\ 0 & 0 \\ \frac{\phi_\pi}{4} & 0 \end{bmatrix} \quad \text{for } i = 1, \dots, 3$$

$$F_t = \begin{bmatrix} 1 - \phi_\pi \delta_t & \phi_\pi \delta_t \\ 0 & 1 \end{bmatrix} \quad O_t = \begin{bmatrix} 1 & \phi_\pi \delta_t \\ 0 & 1 \end{bmatrix} \quad J_t = \begin{bmatrix} 0 & 0 & -\delta_t \\ 0 & 0 & 0 \end{bmatrix}.$$

Stacking up over T yields

$$y = \gamma_y + \gamma_\tau + \Gamma\tau + c \quad (23)$$

$$H_{A,\beta}c = \Lambda\tau + \gamma_c + e, \quad e \sim N(0, \Sigma) \quad (24)$$

$$H_F\tau = \alpha_\tau + Je + Ou, \quad u \sim N(0, \Omega) \quad (25)$$

with

$$\Gamma = \text{blockdiag}([\Gamma'_0, \Gamma'_1]'), \quad O = \text{blockdiag}(O_1, \dots, O_T), \quad J = \text{blockdiag}(J_1, \dots, J_T)$$

$$\Sigma = \text{blockdiag}(\Sigma_1, \dots, \Sigma_T), \quad \Omega = \text{blockdiag}(\Omega_1, \dots, \Omega_T)$$

The impact of initial values is collected in

$$\begin{aligned} \gamma_y &= (\mathbf{1}_T \otimes \tilde{\gamma}_y) \\ \gamma_c &= \left[ \left( \begin{bmatrix} \lambda_1 & \lambda_2 & \dots & \lambda_{q-1} & \lambda_q \\ \lambda_2 & \lambda_3 & \dots & \lambda_q & 0 \\ \vdots & & & & \vdots \\ \lambda_q & 0 & \dots & & 0 \end{bmatrix} \begin{bmatrix} \tau_0 \\ \tau_{-1} \\ \vdots \\ \tau_{-q+1} \end{bmatrix} \right)' \right]_{0_{1 \times (T-q)r}}' \\ \gamma_\tau &= [\Gamma'_1 \tau_0, 0_{1 \times n(T-1)}]' \\ \alpha_\tau &= [(F_1 \tau_0)', 0_{1 \times T(r-1)}]' \end{aligned} \quad (26)$$

and the large coefficient matrices are

$$\begin{aligned}
\Lambda &= \begin{bmatrix} \lambda_0 & 0 & \dots & & & & & 0 \\ \lambda_1 & \lambda_0 & 0 & \dots & & & & 0 \\ & \ddots & \ddots & & \ddots & & & \vdots \\ \lambda_q & \dots & \lambda_1 & \lambda_0 & 0 & \dots & & 0 \\ 0 & \ddots & \ddots & & \ddots & & & \\ \vdots & & & & & & & 0 \\ 0 & \dots & 0 & \lambda_q & \dots & \lambda_1 & \lambda_0 & \end{bmatrix} & H_F &= \begin{bmatrix} I_r & 0 & \dots & & & & & 0 \\ -F_2 & I_r & 0 & \dots & & & & 0 \\ & \ddots & \ddots & & \ddots & & & \vdots \\ 0 & \dots & -F_s & I_r & 0 & \dots & & 0 \\ 0 & \ddots & \ddots & & \ddots & & & \\ \vdots & & & & & & & 0 \\ 0 & \dots & 0 & 0 & \dots & -F_T & I_r & \end{bmatrix} \\
H_{A,\beta} &= \begin{bmatrix} A & 0 & 0 & & & & \dots & 0 \\ -B_1 & A & 0 & & & & \dots & 0 \\ -B_2 & -B_1 & A & 0 & & & \dots & 0 \\ \vdots & & \ddots & \ddots & & & & \vdots \\ -B_p & \dots & & -B_1 & A & 0 & \dots & 0 \\ 0 & \ddots & \ddots & & \ddots & \ddots & & \vdots \\ \vdots & & & & & & A & 0 \\ 0 & \dots & 0 & -B_p & \dots & -B_1 & A & \end{bmatrix}
\end{aligned} \tag{27}$$

## C Bayesian model comparison and estimation of the MCUC

This sections briefly introduces the notation and Bayesian concepts that are useful for understanding the derivation in the next section and the results from model comparison. It draws heavily on Chan and Eisenstat (2015), Chan and Grant (2015), and Chan and Grant (2016).

Let  $M_k$  denote model  $k$  and  $y$  be the data vector. Bayesian model comparison is conducted by a comparison of the marginal data densities or marginal likelihoods (ML)  $p(y|M_k)$  and  $p(y|M_j)$  of models  $k$  and  $j$ . Akin to likelihood ratio tests, the evidence in favor of model  $k$  over model  $j$  is given by the ratio of the marginal likelihoods of the two models, the so-called *Bayes Factor*  $BF_{kj}$ :

$$BF_{kj} = \frac{p(y|M_k)}{p(y|M_j)} \tag{28}$$

The ML of a model is be obtained from prior and posterior densities of the model. To simplify the notation, I omit the the explicit dependence on model  $M_k$  and let  $\theta$  collect all model parameters and let  $p(\theta)$  be the prior density. Then  $p(y|\theta)$  is referred to as the *observed-data* likelihood that is implied by the model equations. The marginal likelihood  $p(y)$  of a model is obtained by integrating out the unknown parameters from the observed data likelihood via

$$p(y) = \int p(y|\theta)p(\theta)d\theta. \quad (29)$$

In most cases, this integral has to be solved numerically, which requires evaluation of  $p(y|\theta)$ . However, for state space models like the MCUC that contain a vector of latent state variables  $\tau$ , the observed-data likelihood  $p(y|\theta)$  cannot readily be evaluated analytically. Instead, only the likelihood  $p(y|\tau, \theta)$  *conditional* on the latent states  $\tau$  can be evaluated directly. To evaluate the observed data, the states  $\tau$  have to be integrated out via

$$p(y|\theta) = \int p(y, \tau|\theta)d\tau = \int p(y|\tau, \theta)p(\tau|\theta)d\tau. \quad (30)$$

where  $p(y, \tau|\theta)$  is called the *complete* data likelihood to distinguish it from the conditional likelihood  $p(y|\tau, \theta)$ . To solve this integral, analytical expressions are available for many linear state space models including the univariate correlated unobserved components model of Grant and Chan (2017). However, to the best of my knowledge, there is no analytical expression for  $p(y|\theta)$  that can suitable for the MCUC. Therefore, in the next section I generalize the results in Grant and Chan (2017) to a multivariate setting. Being able to evaluate  $p(y|\theta)$  analytically enables fast Bayesian model comparison, and Bayesian and maximum likelihood estimation.<sup>18</sup>

## C.1 The observed data density of the MCUC

This section outlines the derivation of  $p(y|\theta)$  and its components. For convenience, I repeat the laws of motions for the vectorized states  $\tau = [\tau'_1, \dots, \tau'_T]'$  and  $c = [c'_1, \dots, c'_T]'$ , and the

---

<sup>18</sup>A less computationally efficient solution would be the Kalman Filter.

observation equation for  $y = [y'_1, \dots, y'_T]'$ :

$$\begin{aligned} y &= \gamma_y + \gamma_\tau + \Gamma\tau + c \\ H_{A,\beta}c &= \Lambda\tau + \gamma_c + e, & e &\sim N(0, \Sigma) \\ H_F\tau &= \alpha_\tau + Je + Ou, & u &\sim N(0, \Omega) \end{aligned}$$

Definitions of the matrices  $H_{A,\beta}$ ,  $H_F$ , and the terms for the initial values are in Appendix B. Note that  $\det(H_{A,\beta}) = \det(H_F) = 1$ . Inverting  $H_{A,\beta}$  and  $H_F$  and absorbing the term involving  $\tau$  from the equation for the cycles  $c$  into the observation equation yields

$$y = \gamma_y + \gamma_\tau + X_{y,\tau}\tau + \tilde{c} \quad (31)$$

$$\tilde{c} = m_{\tilde{c}} + H_{A,\beta}^{-1}e \quad (32)$$

$$\tau = H_F^{-1}\alpha_\tau + H_F^{-1}Je + H_F^{-1}Ou \quad (33)$$

with

$$m_{\tilde{c}} = H_{A,\beta}^{-1}\gamma_c, \quad m_\tau = H_F^{-1}\tilde{\alpha}_\tau, \quad X_{y,\tau} = \Gamma + H_{A,\beta}^{-1}\Lambda.$$

The joint distribution of  $\tilde{c}$  and  $\tau$  is implied by model equations (33) and (32), and reads

$$\begin{aligned} \begin{pmatrix} \tau \\ \tilde{c} \end{pmatrix} &\sim N \left( \begin{pmatrix} m_\tau \\ m_{\tilde{c}} \end{pmatrix}, \begin{pmatrix} H_F^{-1}\Sigma_\tau(H_F^{-1})' & H_F^{-1}\Sigma_{\tau,\tilde{c}}(H_{A,\beta}^{-1})' \\ H_{A,\beta}^{-1}\Sigma'_{\tau,\tilde{c}}(H_F^{-1})' & H_{A,\beta}^{-1}\Sigma_{\tilde{c}}(H_{A,\beta}^{-1})' \end{pmatrix} \right) \\ \text{with } \Sigma_\tau &= O\Omega O' + J\Sigma J' \\ \Sigma_{\tilde{c}} &= \Sigma \\ \Sigma_{\tau,\tilde{c}} &= J\Sigma \end{aligned}$$

This implies the marginal distribution, for  $\tau$  with precision matrix  $K_\tau$  as

$$\tau|\theta \sim N(m_\tau, K_\tau^{-1}) \quad \text{with} \quad K_\tau = H_F'\Sigma_\tau^{-1}H_F \quad (34)$$

and corresponding density function

$$p(\tau|\theta) = (2\pi)^{-\frac{rT}{2}} \det(K_\tau^{-1})^{-\frac{1}{2}} e^{-\frac{1}{2}(\tau-m_\tau)'K_\tau(\tau-m_\tau)}. \quad (35)$$

From the formulas for conditional normal distributions (see e.g. Kroese et al. 2014, Chapter 3.6), the conditional distribution of  $(\tilde{c} | \tau, \theta)$  is

$$\begin{aligned} \tilde{c} | \tau, \theta &\sim N\left(m_{\tilde{c}} + H_{A,\beta}^{-1} B H_F (\tau - m_\tau), K_{\tilde{c}|\tau}^{-1}\right) \\ \text{with } K_{\tilde{c}|\tau}^{-1} &= H_{A,\beta}^{-1} P H_{A,\beta}^{-1'} \\ B &= \Sigma'_{\tau, \tilde{c}} \Sigma_\tau^{-1} = \Sigma J' (O \Omega O' + J \Sigma J')^{-1} \\ P &= \Sigma - \Sigma J' (O \Omega O' + J \Sigma J')^{-1} J \Sigma \end{aligned} \quad (36)$$

In the case of constant variances and learning gain  $\delta$ , the matrices  $O$ ,  $J$ ,  $\Omega$  and  $\Sigma$  have a Kronecker structure and the expressions for  $B$  and  $P$  could be further simplified. To handle breaks in variances I stick to the more general expressions in this derivation. The distribution in (36) and the observation equation (31) together imply the condition distribution  $(y | \tau, \theta)$

$$\begin{aligned} y | \tau, \theta &\sim N\left(m_{y,\tau} - H_{A,\beta}^{-1} B H_F m_\tau + X \tau, K_{y|\tau}^{-1}\right) \\ \text{with } m_{y,\tau} &= \gamma_y + H_{A,\beta}^{-1} \gamma_c + \gamma_\tau \\ X &= H_{A,\beta}^{-1} B H_F + \Gamma + H_{A,\beta}^{-1} \Lambda \\ K_{y|\tau} &= K_{\tilde{c}|\tau} = H'_{A,\beta} P^{-1} H_{A,\beta} \end{aligned} \quad (37)$$

with the corresponding conditional data density

$$p(y | \tau, \theta) = (2\pi)^{-\frac{nT}{2}} \det(K_{y|\tau}^{-1})^{-\frac{1}{2}} e^{-\frac{1}{2}(y - m_{y,\tau} - X\tau)' K_{y|\tau} (y - m_{y,\tau} - X\tau)}. \quad (38)$$

The complete data density  $p(y, \tau | \theta)$  is obtained as the product of the two densities in  $p(\tau | \theta)$  in (35) and  $p(y | \tau, \theta)$  in (38). Applying the steps in the appendix of Grant and Chan (2017) to solve the integral in (30) yields the observed data density  $p(y | \theta)$ . To that end, define  $c_1 = (2\pi)^{-\frac{(n+r)T}{2}} \det(K_{y|\tau}^{-1})^{-\frac{1}{2}} \det(K_\tau^{-1})^{-\frac{1}{2}}$  and rewrite

$$\begin{aligned} p(y | \theta) &= \int p(y, \tau | \theta) d\tau = \int p(y | \tau, \theta) p(\tau | \theta) d\tau \\ &= c_1 \int e^{-\frac{1}{2}[(y - m_{y,\tau} - X\tau)' K_{y|\tau} (y - m_{y,\tau} - X\tau) + (\tau - m_\tau)' K_\tau (\tau - m_\tau)]} d\tau \end{aligned}$$

After some algebra, the observed data density can be written as

$$= (2\pi)^{-\frac{nT}{2}} \det(K_{y|\tau}^{-1})^{-\frac{1}{2}} \det(K_\tau^{-1})^{-\frac{1}{2}} \det(P_\tau^{-1})^{\frac{1}{2}} e^{-\frac{1}{2}[(y - m_{y,\tau})' K_{y|\tau} (y - m_{y,\tau}) + m_\tau' K_\tau m_\tau - d_\tau' P_\tau^{-1} d_\tau]}.$$

with  $P_\tau = X'K_{y|\tau}X + K_\tau$  and  $d_\tau = X'K_{y|\tau}(y - m_{y,\tau}) + K_\tau m_\tau$ . This expression does not depend on the states  $\tau$  anymore and thus, be evaluated directly. I employ this expression in the estimation of the marginal data density of the MCUC using the cross-entropy method of Chan and Eisenstat (2015).

## C.2 Drawing the states $\tau$

A by product of this derivation is an analytical expression for  $p(y, \tau | \theta)$ . Bayes' formula shows that the full conditional posterior  $p(\tau | y, \theta)$  is proportional to  $p(y, \tau | \theta)$ .

$$\begin{aligned} p(\tau | y, \theta) &= \frac{p(y | \tau, \theta)p(\tau | \theta)}{p(y)} \\ &\propto p(y | \tau, \theta)p(\tau | \theta) = p(y, \tau | \theta) \end{aligned}$$

Then, from the above derivation it follows that

$$p(\tau | y, \theta) \propto e^{-\frac{1}{2}[(\tau - P_\tau^{-1}d_\tau)'P_\tau(\tau - P_\tau^{-1}d_\tau)]}.$$

This is the kernel of the multivariate normal distribution  $N(\hat{\tau}, P_\tau^{-1})$  with  $\hat{\tau} = P_\tau^{-1}d_\tau$ . The precision sampler of Chan and Jeliazkov (2009) can be used to generate draws of  $\tau$  in a Gibbs sampler that simulates the posterior of the entire model.

## D Gibbs sampler for the MCUC with breaks in variances and the learning rate

This section presents the details of the Gibbs sampler for the baseline model with breaks in the shock variances and the learning rate. To that end, let

$$\theta = \{A, \beta, \delta, \bar{g}, rr, d, \sigma_g^2, \sigma_\pi^2, \sigma_{MP}^2, \sigma_P^2, \sigma_\star^2, \sigma_{LR}^2\}$$

collect all parameters that make up the model matrices and let  $\theta_{-i}$  be all parameters except parameter set  $i$ . The Gibbs sampler to estimate the model in (23) to (25) will consists of iteration of the following steps:

1. Sample  $\tau$  jointly.
2. Sample the free parameters in  $\gamma_y$  and  $\tilde{\Gamma}$ .

3. Sample the free parameters in  $\beta$  and  $\lambda$  equation by equation, subject to stability of the cycles.
4. Sample  $\delta$ , the parameter in the trend equation.
5. Sample the shock variances  $\Sigma$  and  $\Omega$ .
6. Sample the  $p$  initial values  $\tau_0$ .

Each parameter block is sampled from its full conditional posterior density. The following presents the details of the densities for each step.

**1. Sampling the states  $\tau$  jointly.** A by product of the derivation of the marginal data density of the MCUC in Appendix C.1 is an analytical expression for  $p(y, \tau | \theta)$ . Bayes' formula shows that the full conditional posterior  $p(\tau | y, \theta)$  is proportional to  $p(y, \tau | \theta)$ .

$$\begin{aligned} p(\tau | y, \theta) &= \frac{p(y | \tau, \theta)p(\tau | \theta)}{p(y)} \\ &\propto p(y | \tau, \theta)p(\tau | \theta) = p(y, \tau | \theta) \end{aligned}$$

It follows that

$$p(\tau | y, \theta) \propto e^{-\frac{1}{2}[(\tau - P_\tau^{-1}d_\tau)'P_\tau(\tau - P_\tau^{-1}d_\tau)]}.$$

This is the kernel of the multivariate normal distribution  $N(\hat{\tau}, P_\tau^{-1})$  with  $\hat{\tau} = P_\tau^{-1}d_\tau$ . The precision sampler of Chan and Jeliazkov (2009) can be used to generate draws of  $\tau$  in a Gibbs sampler that simulates the posterior of the entire model.

**2. Sampling the parameters in the observation equation.**

To account for linear restrictions on free the parameters in the constants  $\tilde{\gamma}_y$  and factor loadings  $\tilde{\Gamma}$ , jointly denoted as  $\bar{\gamma} = \text{vec}([\tilde{\gamma}_y, \Gamma_0, \Gamma_1]')$ , let the  $\bar{\gamma}_f$  collect the free elements that are related to  $\bar{\gamma}$  via

$$\bar{\gamma} = R_\gamma \bar{\gamma}_f + r_\gamma.$$

In the present model,  $\bar{\gamma}_f = [\bar{g}, rr']'$ . The posterior of  $\gamma_f$  is given by

$$p(\gamma_f | y, \tau, \theta_{-\gamma_f}) \propto p(y | \tau, \theta)p(\gamma_f)$$

$\gamma_f$  appears in the observation equation (23). Plugging in (24) and collecting terms to write in terms of the correlated errors  $e$  yields

$$y = \gamma_y + \gamma_\tau + (\Gamma + H_{A,\beta}^{-1}\Lambda)\tau + H_{A,\beta}^{-1}e.$$

Define  $\gamma_\tau + \gamma_y + \Gamma\tau = \tilde{X}_\gamma\bar{\gamma}$  to factor out  $\bar{\gamma}$  yields

$$\begin{aligned} y &= H_{A,\beta}^{-1}\Lambda\tau + \tilde{X}_{y\gamma}\bar{\gamma} + \tilde{c} \\ \text{with } \tilde{X}'_\gamma &= [x_{y\tau,1}, \dots, x_{y\tau,T}]' \quad \text{and} \quad x'_{y\tau,t} = I_n \otimes [1 \ \tau'_t \ \tau'_{t-1}]. \end{aligned}$$

Inserting the linear restrictions for  $\bar{\gamma}$  implies the following conditional likelihood via (37) in terms of the free parameters  $\bar{\gamma}_f$

$$\begin{aligned} y|\theta, \tau &\sim N(m_{y,\gamma} + X_{y\gamma}\bar{\gamma}_f, K_{y|\tau}^{-1}) \\ \text{with } m_{y,\gamma} &= H_{A,\beta}^{-1}(BH_F\tau - B\alpha_\tau) + \tilde{X}_\gamma r_\gamma + H_{A,\beta}^{-1}(\Lambda\tau + \gamma_c) \\ \text{and } X_\gamma &= \tilde{X}_\gamma R_\gamma \end{aligned}$$

Combining this conditional likelihood with a normal prior  $\gamma_f \sim N(a_\gamma, V_\gamma)$  yields the posterior via standard regression results:

$$\begin{aligned} \gamma_f|y, \theta, \tau &\sim N(\hat{\gamma}_f, K_\gamma^{-1}) \\ \text{with } K_\gamma &= V_\gamma^{-1} + X'_\gamma K_{y|\tau} X_\gamma \\ \text{and } \hat{\gamma}_f &= K_\gamma^{-1} (V_\gamma^{-1} a_\gamma + (H_{A,\beta} X_\gamma)' P^{-1} y_\gamma^*) \end{aligned} \tag{39}$$

where  $y_\gamma^* = H_{A,\beta}(y - m_{y,\gamma}) = H_{A,\beta}(y - \tilde{X}_\gamma r_\gamma) - (BH_F + \Lambda)\tau - \gamma_c - B\alpha_\tau$ .

### 3. Sampling the free coefficients in $A$ , $B_1, \dots, B_p$ and $\Lambda$

The coefficients in the cycles and  $\tau$  are connected via linear cross equation restrictions due to the learning mechanism. Therefore, they must be sampled jointly. Since  $A$  is recursive, the equation for in  $c$  can be written as a system of equations by bringing  $A$  to the right hand side as follows:

$$c_t = -(A - I_n)c_t + B_1 c_{t-1} + \dots + B_p c_{t-p} + \lambda_0 \tau_t + \dots + \lambda_q \tau_{t-q} + e_t, \quad e_t \sim N(0, \Sigma). \tag{40}$$

Due to the recursive structure in  $A$ , the term  $-(A - I_n)c_t$  does not introduce dependence of  $c_{it}$  to itself. Next, let  $\beta$  collect the free elements in vectorized form. They appear in the

vectorized equations for  $c$  in for following way

$$c = X_c R_{c,\beta} \beta + e \quad (41)$$

$$\text{with } R_{c,\beta} \beta = \left[ \text{vec}(-(A - I_n))' \quad \text{vec}([B_1 \dots B_p])' \quad \text{vec}([\lambda_0 \dots \lambda_q])' \right]' \quad (42)$$

and with a total of  $n_A = \frac{n(n-1)}{2}$  parameters in the recursive  $A$  matrix and  $(i-1)$  parameters in the  $i$ th row. Additionally, equation  $i$  contains  $np$  parameters in the  $B$  matrices each  $qr$  parameters in the  $\lambda$ s. In total there are  $n_B = n^2 p$  and  $n_\lambda = nqr$  parameters in the  $B$ 's  $\lambda$ s. However, these parameters are subject to restrictions such that the number of free elements in  $\beta$  in equation  $i$  is denoted  $k_i$ . Let the total number of free parameters be  $K = \sum_{i=1}^n k_i$ . Since only the monetary policy equation is restricted and only the  $\lambda$ s in this equation contain non-zero elements,  $k_i$  equals the total number of parameters per equation for the first two equations. Thus, we have  $k_i = np$  for  $i < 3$ . Furthermore,  $k_3 = 1$  because the only free element on lagged variables in the third equation is the interest rate smoothing parameter. Hence, the total number of free parameters is  $K_\beta = n_A + K$  and  $R_{c,\beta}$  can be written as follows

$$R_{c,\beta} = \begin{bmatrix} & & 0_{n_A \times K} \\ & R_{A,\beta} & R_{B,\beta} \\ n(np + \frac{(n-1)}{2} + qr) \times K_\beta & & 0_{n_\lambda \times K} \end{bmatrix} \quad (43)$$

$$R_{B,\beta} = \begin{bmatrix} I_{np} & 0_{np \times k_2} & 0_{np \times k_3} \\ 0_{np \times k_1} & I_{np} & 0_{np \times k_3} \\ 0_{np \times k_1} & 0_{np \times k_2} & R_{B,\rho} \\ & & np \times 1 \end{bmatrix} \quad (44)$$

The only non-zero element in  $R_{B,\rho}$  is a one in column  $n$ . The only linear restriction concerns the monetary policy reaction coefficient to inflation  $\phi_\pi$ .  $\phi_\pi$  appears in  $A$  as well as in the  $B$ 's and  $\lambda$ 's. Therefore

$$R_{A,\beta} = \begin{bmatrix} I_{n_A-1} & \\ 0_{n^2 p \times n_A} & R_{\phi_\pi, \beta} \\ 0_{nqr \times n_A} & \end{bmatrix}$$

with the column vector of  $R_{\phi_\pi, \beta}$  of size  $n(np + \frac{(n-1)}{2} + qr) \times 1$ .  $R_{\phi_\pi, \beta}$  has 0.25 at positions  $n_A$  and  $n_A + k_1 + k_2 + 2 + (j-1)n$  for  $j = 1, \dots, p-1$  for the contemporaneous and lagged reaction to the inflation gap (i.e. 4-period average), at positions  $n_A + K + i_{\pi^p} + (j-1)r$

for the reaction to the 4-period average of  $\pi^P$  and, finally,  $-1$  at position  $n_A + K + r$  for the reaction to  $\pi_t^*$ , where  $\pi_t^*$  is ordered last within the trends  $\tau$ ).

$\phi_\pi$ , which is part of the coefficient vector  $\beta$ , also appears in the law of motion for  $\tau$ . Due to the upper triangular structure of  $O_t$  it hold that  $O_t^{-1}F_t = \begin{bmatrix} 1 & -\phi_\pi\delta_t \\ 0 & 1 \end{bmatrix} \begin{bmatrix} 1 - \phi_\pi\delta_t & \phi_\pi\delta_t \\ 0 & 1 \end{bmatrix} = \begin{bmatrix} 1 - \phi_\pi\delta_t & 0 \\ 0 & 1 \end{bmatrix}$  so the law of motion can be rewritten as

$$\begin{aligned} O_t^{-1}\tau_t &= \tau_{t-1} + J_t e_t + u_t \\ \tau_t &= -(O_t - I)\tau_{t-1} + J_t e_t + u_t \end{aligned}$$

For deriving the posterior of  $\beta$  rewrite the law of motion for the trends as

$$\begin{aligned} \tau &= X_\tau(R_{\tau,\beta}\beta + r_{\tau,\beta}) + (I_t \otimes J)e + (I_T \otimes O)u \\ \text{with } X_\tau &= [x'_{\tau,1}, \dots, x'_{\tau,T}] \\ \text{and } x_{\tau,t} &= I_2 \otimes [\tau'_t, \tau'_{t-1}] \end{aligned}$$

The full conditional posterior density of  $\beta$  denoted  $p(\beta|y, \tau, \theta_{-\beta})$  is, thus, obtained by

$$\begin{aligned} p(\beta|y, \tau, \theta_{-\beta}) &\propto p(c, \tau | \beta, \theta_{-\beta})p(\beta) \\ &= p(c | \tau, \beta, \theta_{-\beta})p(\tau | \beta, \theta_{-\beta})p(\beta). \end{aligned}$$

I proceed by first deriving the marginal distribution of  $\tau$ , denoted  $p(\tau|\beta, \theta_{-\beta})$ , and then the conditional distribution of  $c$ , denoted  $p(c|\tau, \beta, \theta_{-\beta})$ , from joint distribution of  $\tau$  and  $c$ . The joint distribution of  $c$  and  $\tau$  is given by

$$\begin{aligned} \begin{pmatrix} \tau \\ c \end{pmatrix} &\sim N \left( \begin{pmatrix} X_\tau(R_{\tau,\beta}\beta + r_{\tau,\beta}) \\ X_c R_{c,\beta}\beta \end{pmatrix}, \begin{pmatrix} \Sigma_\tau & \Sigma_{\tau,\tilde{c}} \\ \Sigma_{\tau,\tilde{c}} & \Sigma_{\tilde{c}} \end{pmatrix} \right) \\ \text{with } \Sigma_\tau &= O\Omega O' + J\Sigma J' \\ \Sigma_{\tilde{c}} &= \Sigma \\ \Sigma_{\tau,\tilde{c}} &= J\Sigma \end{aligned}$$

Therefore, the marginal distribution of  $\tau$  is

$$\tau \sim N(X_\tau(R_{\tau,\beta}\beta + r_{\tau,\beta}), \Sigma_\tau).$$

Applying the formulas for conditional normal distributions, the distribution of  $c$  conditional on  $\tau$  is found as

$$\begin{aligned}
c | \tau, \theta &\sim N\left(X_\beta \beta + m_{c,\beta}, K_{c|\tau}^{-1}\right) \\
\text{with} \quad X_\beta &= X_c R_c - B X_\tau R_\tau \\
m_{c,\beta} &= B(\tau - X_\tau r_{\tau,\beta}) \\
B &= \Sigma'_{\tau,\tilde{c}} \Sigma_\tau^{-1} \\
K_{c|\tau}^{-1} &= \Sigma_{\tilde{c}} - \Sigma'_{\tau,\tilde{c}} \Sigma_\tau^{-1} \Sigma_{\tau,\tilde{c}} \\
&= P
\end{aligned}$$

Combining the densities with the with the normal prior  $\beta \sim N(\beta_0, V_\beta)$  via Bayes' rule yields the following posterior:

$$\begin{aligned}
\beta | y, \tau, \theta_{-\beta} &\sim N(\hat{\beta}, K_\beta^{-1}) \\
\text{with} \quad K_\beta &= V_\beta^{-1} + X'_\beta K_{c|\tau} X_\beta + (X_\tau R_{\tau,\beta})' K_\tau X_\tau R_{\tau,\beta} \\
\text{and} \quad \hat{\beta} &= K_\beta^{-1} \left( V_\beta^{-1} \beta_0 + X'_\beta K_{c|\tau} (c - m_{c,\beta}) + (X_\tau R_{\tau,\beta})' K_\tau (\tau - X_\tau r_{\tau,\beta}) \right)
\end{aligned} \tag{45}$$

#### 4. Sampling $\delta$

The learning rate  $\delta_t$  appears only in the law of motion for the perceived target. One complication arises because  $\delta_t > 0$  for each regime. To account for this inequality restriction, the parameter can be sampled with a Griddy Gibbs step. The Griddy Gibbs step requires a closed interval. Therefore, to apply it to the sampling of  $\delta_t$ , I implement an upperbound  $\delta_t < \delta_{\text{ub}}$  that is large enough that it does not constrain the estimate for  $\delta$  in the empirical application. The Griddy Gibbs step also requires the full conditional posterior of  $\delta_t$ . To that end, rewrite the law of motion for  $\pi_t^P$

$$\begin{aligned}
\pi_t^P &= (1 - \delta_t \phi_\pi) \pi_{t-1}^P + \delta_t \phi_\pi \pi_t^* - \delta_t \varepsilon_t^{MP} + \varepsilon_t^P \\
\text{from (6) as} \quad \pi_t^P &= X_\delta (R_\delta \delta + r_\delta) + \varepsilon_t^P \\
\text{with} \quad X_\delta &= \left[ [\pi_0^P, \pi_{[1:T-1]}^P]', \pi^*, \varepsilon_t^{MP} \right]
\end{aligned}$$

where  $\pi_{[1:T-1]}^P$  are the elements of  $\pi^P$  from  $t = 1$  to  $t = T-1$ . The vectors  $R_\delta = [-\phi_\pi, \phi_\pi, -1]'$  and  $r_\delta = [1, 0, 0]'$  account for the linear restrictions on  $\delta_t$ . The conditional likelihood implied by this equation is  $\pi_P | \tau, \theta_{-\delta} \sim N(X_\delta (R_\delta \delta + r_\delta), \sigma_P^2)$ . The posterior is obtained by mul-

tipling this density with the beta prior distribution. The resulting conditional posterior has bounded support. To generate a draw of  $\delta$  from this distribution, the density is first evaluated on a fine grid for values of  $\delta$ . A draw is then generated with the inverse-transform method.

## 5. Sampling the shock variances

Since the inverse Gamma priors for the variances are conjugate, it is straight forward to sample them from their full conditional distributions. Conditional on the  $\tau$  and all parameters except for the variances, the errors are obtained via the model relations. For simplicity denote all shocks  $\varepsilon = [\varepsilon^g, \varepsilon^\pi, \varepsilon^{MP}, \varepsilon^P, \varepsilon^\star]$ . Then, the  $i$ th for  $i = g, \pi, MP, P, \star$  shock in regime  $m = 1, \dots, M$  is denoted  $\varepsilon_{i,m}$ . The corresponding prior for each  $\sigma_{i,m}^2$  is  $\sigma_{i,m}^2 \sim IG(\nu_i, S_i)$ . Note that the priors are not regime specific. The full conditional posterior is obtained from standard conjugate results:

$$\sigma_{i,m}^2 | \tau, \theta_{-\sigma_{i,m}^2} \sim IG\left(\frac{T_m}{2} + \nu_i, S_i + 0.5\varepsilon'_{i,m}\varepsilon_{i,m}\right)$$

where  $T_m$  is the number of observations in regime  $m$ . All variances are sampled individually from their posteriors consecutively.

## 6. Sampling the initial values $\tau_0$

The initial values for the states  $\tau_0$  appear in two places in the model: In the observation equation and in the law of motion for the first  $\tau$  at  $t = 1$ , denoted  $\tau_1$ . Therefore, the full conditional posterior is given by:

$$p(\tau_0 | y, \tau, \theta_{-\tau_0}) \propto p(y | \tau, \theta) p(\tau_1 | \theta) p(\tau_0)$$

where  $\theta_{-\tau_0}$  collects all model parameters except the initial states  $\tau_{[0:1-q]}$ . Note that in the density  $p(y | \tau, \theta)$  up to  $q$  pre-sample values for  $\tau$  will appear through via the Taylor rule. For sampling  $\tau_0$ , I make a simplifying assumption that all values in further pre-sample periods are equal to the value at  $t = 0$ , i.e.  $\tau_{-s} = \tau_0$  for  $s \geq 1$ . Derivation of  $p(y | \tau, \theta)$  follows from the observation equation where  $c$  was inserted

$$y = \gamma_y + \gamma_\tau + H_{A,\beta}^{-1}\gamma_c + (\Gamma + H_{A,\beta}^{-1}\Lambda)\tau + H_{A,\beta}^{-1}e. \quad (46)$$

Redefine the following expressions

$$\gamma_c = \gamma_{c,\tau_0} \tau_0 = \left[ \left( \begin{bmatrix} \lambda_1 & \lambda_2 & \dots & \lambda_{q-1} & \lambda_q \\ \lambda_2 & \lambda_3 & \dots & \lambda_q & 0 \\ \vdots & & & & \vdots \\ \lambda_q & 0 & \dots & & 0 \end{bmatrix} \begin{bmatrix} \mathbf{1}_{r \times r} \\ \mathbf{1}_{r \times r} \\ \vdots \\ \mathbf{1}_{r \times r} \end{bmatrix} \right)' \mathbf{0}_{r \times (T-q)n} \right]' \tau_0 \quad (47)$$

$$\gamma_\tau = \gamma_{\tau,\tau_0} \tau_0 = [\Gamma'_1, \mathbf{0}_{r \times n(T-1)}]' \tau_0 \quad (48)$$

$$\alpha_\tau = [F', \mathbf{0}_{r \times n(T-1)}]' \tau_0 \quad (49)$$

and factoring out  $\tau_0$  gives

$$y = \gamma_y + \left( \gamma_{\tau,\tau_0} + H_{A,\beta}^{-1} \gamma_{c,\tau_0} \right) \tau_0 + \left( \Gamma + H_{A,\beta}^{-1} \Lambda \right) \tau + H_{A,\beta}^{-1} e.$$

Using this reformulation in the conditional distribution in Equation (??) implies following conditional likelihood

$$\begin{aligned} y | \tau_0, \tau, \theta &\sim N(m_{y,\tau_0} + X_{y0} \tau_0, K_{y|\tau}^{-1}) \\ \text{with} \quad m_{y,\tau_0} &= \gamma_y + (\Gamma + H_{A,\beta}^{-1} \Lambda + H_{A,\beta}^{-1} B) \tau = \gamma_y + X_{y\tau} \tau \\ \text{and} \quad X_{y,\tau_0} &= \gamma_{\tau,\tau_0} + H_{A,\beta}^{-1} (\gamma_{c,\tau_0} - B[F', \mathbf{0}_{r \times n(T-1)}]') \end{aligned} \quad (50)$$

Additionally, the initial values appear in the of motion for  $\tau_t$  at  $t = 1$ :

$$\tau_1 = F_1 \tau_0 + J_1 e_1 + O_1 u_1 \quad (51)$$

which implies the distribution (marginal of  $y$ )  $\tau_1 | \theta \sim N(F_1 \tau_0, K_{\tau_1}^{-1})$  with precision matrix  $K_{\tau_1} = (J_1 \Sigma_1 J'_1 + O_1 \Omega_1 O'_1)^{-1}$ . Combining these two densities with a normal prior  $\tau_0 \sim N(a_0, B_0)$  yields the following conditional posterior:

$$\begin{aligned} \tau_0 | y, \tau, \theta_{-\tau_0} &\sim N(\hat{\tau}_0, K_{\tau_0}^{-1}) \\ \text{with} \quad K_{\tau_0} &= B_0^{-1} + F' K_{\tau_1} F + (H_{A,\beta} X_{y0})' P_\tau^{-1} H_{A,\beta} X_{y0} \\ \text{and} \quad \hat{\tau}_0 &= P_{\tau_0}^{-1} \left( B_0^{-1} a_0 + F' K_{\tau_1} \tau_1 + (H_{A,\beta} X_{y0})' P^{-1} H_{A,\beta} (y - m_{y,\tau_0}) \right) \\ &= P_{\tau_0}^{-1} \left( B_0^{-1} a_0 + F' K_{\tau_1} \tau_1 + (H_{A,\beta} X_{y0})' P^{-1} H_{A,\beta} (y - \gamma_y - (\Gamma + H_{A,\beta}^{-1} \Lambda + H_{A,\beta}^{-1} B) \tau) \right) \\ &= P_{\tau_0}^{-1} \left( B_0^{-1} a_0 + F' K_{\tau_1} \tau_1 + (H_{A,\beta} X_{y0})' P^{-1} [H_{A,\beta} (y - \gamma_y - \Gamma \tau) - (\Lambda + B) \tau] \right) \end{aligned} \quad (52)$$

**Diskussionsbeiträge - Fachbereich Wirtschaftswissenschaft - Freie Universität Berlin**  
**Discussion Paper - School of Business & Economics - Freie Universität Berlin**

2022 erschienen:

- 2022/1 AHRENS, Steffen; Ciril BOSCH-ROSA und Thomas MEISSNER:  
Intertemporal Consumption and Debt Aversion: A Replication and Extension  
*Economics*
- 2022/2 WOLF, Elias: Estimating Growth at Risk with Skewed Stochastic Volatility  
Models  
*Economics*
- 2022/3 GLAUBITZ, Rick; Astrid HARNACK-EBER und Miriam WETTER: The Gender  
Gap in Lifetime Earnings: the Role of Parenthood  
*Economics*
- 2022/4 RENDTEL, Ulrich und Juha ALHO: On the Fade-away of an Initial Bias in  
Longitudinal Surveys  
*Economics*
- 2022/5 COLEMAN, Winnie und Dieter NAUTZ: Inflation Target Credibility in Times of  
High Inflation  
*Economics*
- 2022/6 BESTER, Helmut und József SÁKOVICS: Cooperation, Competition, and  
welfare in a matching market  
*Economics*
- 2022/7 JABAKHANJI, Samira; Anthony LEPINTEUR; Giorgia MENTA; Alan PIPER und  
Claus VÖGELE: Sleep Quality and the Evolution of the COVID-19 Pandemic in  
Five European Countries  
*Economics*
- 2022/8 AHRENS, Steffen und Ciril BOSCH-ROSA: Motivated Beliefs, Social  
Preferences, and Limited Liability in Financial Decision-Making  
*Economics*